40p

NASA TN D-1885

TECHNICAL NOTE
D-1885

STUDY OF THE NONEQUILIBRIUM FLOW FIELD BEHIND NORMAL SHOCK WAVES IN CARBON DIOXIDE

By John T. Howe, John R. Viegas,
and Yvonne S. Sheaffer

Ames Research Center
Moffett Field, Calif.

NATIONAL AERONAUTICS AND SPACE ADMINISTRATION
WASHINGTON
June 1963

0 1

NATIONAL AERONAUTICS AND SPACE ADMINISTRATION

TECHNICAL NOTE D-1885

STUDY OF THE NONEQUILIBRIUM FLOW FIELD BEHIND NORMAL SHOCK WAVES IN CARBON DIOXIDE[1]

By John T. Howe, John R. Viegas,
and Yvonne S. Sheaffer

SUMMARY

Chemical reaction rate coefficients for the dissociation of CO_2 and CO are estimated by use of collision theory and are compared with experimental results obtained at low temperatures. The effect of varying the number of square terms of energy effective in collisions on the rate coefficients is examined. The estimated rate coefficients are employed to study the interdependent chemical rate processes for the dissociation of CO_2 and its components (including five chemical species) coupled with the fluid flow behind a normal shock wave. Solutions of the differential equations are obtained for shock speeds up to 10 km/sec at 10^{-2} to 10^{-4} standard atmospheric density by three methods. Thus results of two simplified methods (one of which leads to a closed form solution) are compared with those of an exact method. Chemical relaxation effects for shock waves in CO_2 are compared with those in N_2 and O_2. Results for CO_2 are presented in the form of flow-field profiles of pressure, temperature, density, enthalpy, and species concentration, and in the form of a relaxation distance behind the shock as a function of shock speed and ambient density.

INTRODUCTION

Entry into planetary atmospheres having CO_2 components enhances the interest in the dissociative reactions of CO_2. Although the estimated CO_2 concentration in planetary atmospheres is not large (estimates by Kaplan (ref. 2) are of the order of 10 percent for Venus and less than that for Mars), it is important to understand the chemical kinetics for CO_2 dissociation as well as for mixtures of CO_2 with other gases.

---

[1]This study has also been discussed in reference 1. The information contained in that paper has been considerably expanded in the present work. Additional discussion of physical phenomena, methods of solution, and additional results are included in this paper.

A considerable amount of work has been done on phenomena in CO_2 in chemical equilibrium related to planetary atmosphere entry. For example, Yee, Bailey, and Woodward (ref. 3) have measured the heat transfer and have made equilibrium shock-wave calculations in CO_2; Thomas (ref. 4) has estimated the transport properties for equilibrium CO_2; Hoshizaki (ref. 5) has calculated the heat transfer for high-speed flight in pure CO_2 assuming chemical equilibrium in the flow field; and Woodward (ref. 6) has calculated the equilibrium properties behind normal shocks in CO_2 - N_2 mixtures.

In the present paper, attention is focused on the nonequilibrium dissociative relaxation of CO_2 behind a normal shock wave. Our purpose is to estimate the nonequilibrium chemical effects on a dissociating CO_2 flow field. The results are of interest for CO_2 shock-tube and wind-tunnel studies and are useful as a first step in studying nonequilibrium effects in gas mixtures containing a CO_2 component.

At present, the reaction rate coefficients for CO_2 dissociation are not well known. Although Brabbs, Belles, and Zlatarich (in work not yet published) and Gaydon and Hurle (ref. 7) have obtained some experimental results at relatively low temperatures, very little is known about the reactions or their rate coefficients at the high temperatures behind strong shock waves. For that reason, the reactions are postulated and their rates are estimated in this paper.

SYMBOLS

A Avogadro's number

a defined by equation (45)

a_{zi} number of atoms of type z in species i

Bc_r coefficient in equilibrium coefficient expression (23) for reaction r

Bf_r coefficient in forward reaction rate coefficient expression (22) for reaction r

$\hat{c}_{p_i}$ specific heat at constant pressure for species i on a "per mole" basis

$\bar{d}$ average diameter of two colliding particles

Ec_r energy in equilibrium coefficient expression (23) for reaction r

Ef_r activation energy in forward reaction rate coefficient expression (22) for reaction r

h static enthalpy (per mass basis)

$\hat{h}$ static enthalpy (per mole basis)

$\hat{h}_i^o$ enthalpy of formation of species i (per mole basis)

K_{c_r} equilibrium coefficient for reaction r

k_{f_r} forward reaction rate coefficient for reaction r

k total number of species (eq. (7))

M "typical" collision partner and molecular weight

M* reduced molecular weight $(1/M_i + 1/M_M)^{-1}$

n_i number of moles of species i per unit mass of mixture

P transition probability or frequency factor

p static pressure

$\hat{R}$ universal gas constant

s number of classical squared terms of energy contributing to reaction

T absolute temperature

u velocity in x direction

X species

x distance behind shock

α forward stoichiometric coefficient, and exponent in equations (22) and (23)

β backward stoichiometric coefficient

ϵ $\frac{\rho_\infty}{\rho_s}$ density ratio across shock wave

η defined by equation (51)

ρ mass density of mixture

ρ_o standard or sea level atmosphere density (1.225×10^{-3} g/cm^3)

σ constant in equation (21)

Superscripts

^ per mole basis

- equilibrium value

Subscripts

a	location of point in sketch (b)
b	backward
eq	equilibrium value
f	forward
i	species i; i = 1 through 5 corresponds to CO_2, CO, O_2, O, and C, respectively
M	pertaining to the typical collision partner
o	reference condition at sea level
r	rth reaction; r = 1 through 3 shown in equations (18) through (20)
s	conditions immediately behind shock
∞	conditions ahead of shock

ANALYSIS

Differential Equations

The flow model chosen for analysis is that of a normal shock moving at velocity u_∞ into quiescent CO_2 at density ρ_∞. The corresponding flow field as seen by an observer traveling with the shock is shown in sketch (a).

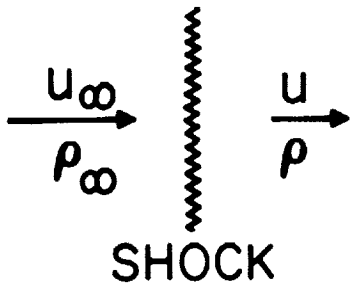

Sketch (a).- Flow model.

The equations describing the flow field behind the shock are (neglecting transport phenomena)

$$\rho u = \rho_\infty u_\infty = \text{constant} \tag{1}$$

$$\rho u(du/dx) = -(dp/dx) \tag{2}$$

$$u\,du + dh = 0 \tag{3}$$

where enthalpy of the mixture of species is

$$h(p,\rho,n_1 \ldots n_k) = \sum_{i=1}^{k} n_i \hat{h}_i \tag{4}$$

and

$$\hat{h}_i = \int_o^T \hat{c}_{p_i}\, dT + \hat{h}_i^{\,o} \tag{5}$$

It is noted on the left side of equation (4) that h is assumed to be a function of pressure, density, and chemical composition but not of the vibrational state of the molecules. Thus we neglect vibrational relaxation in favor of chemical relaxation (the former being fast compared with the latter for CO_2, according to reference 7, at temperatures up to 2700° K). The advantage of this simplification will be apparent subsequently when we consider specific heat. The equation of state of the mixture is

$$p = \rho \hat{R} T \sum_{i=1}^{k} n_i \tag{6}$$

Equations (1), (2), (3), and (4) can be combined to yield (ref. 8)

$$\frac{du}{u} = \frac{\dfrac{1}{\rho(\partial h/\partial \rho)} \displaystyle\sum_{i=1}^{k} \frac{\partial h}{\partial n_i}\, dn_i}{1 - u^2 \left[\dfrac{(\partial h/\partial p) - (1/\rho)}{-(\partial h/\partial \rho)}\right]} \tag{7}$$

which is readily put into the form

$$\frac{du}{dx} = \frac{u}{1 - \dfrac{\rho u^2}{p} \dfrac{\displaystyle\sum_{i=1}^{k} n_i \left(\frac{\hat{c}_{p_i}}{\hat{R}} - 1\right)}{\displaystyle\sum_{i=1}^{k} n_i \frac{\hat{c}_{p_i}}{\hat{R}}}} \left(\frac{\displaystyle\sum_{i=1}^{k} \frac{dn_i}{dx}}{\displaystyle\sum_{i=1}^{k} n_i} - \frac{\displaystyle\sum_{i=1}^{k} \frac{\hat{c}_{p_i}}{\hat{R}} \frac{dn_i}{dx}}{\displaystyle\sum_{i=1}^{k} n_i \frac{\hat{c}_{p_i}}{\hat{R}}} - \frac{\displaystyle\sum_{i=1}^{k} \hat{h}_i^{\,o} \frac{dn_i}{dx}}{\hat{R}T \displaystyle\sum_{i=1}^{k} n_i \frac{\hat{c}_{p_i}}{\hat{R}}} \right) \tag{8}$$

where it is assumed for the sake of simplicity that $\hat{c}_{p_i}/\hat{R}$ is constant at its fully excited classical value (5/2 for atoms, 9/2 for diatomic molecules, and 7 for triatomic molecules (ref. 9)).

Thus flow equations (1) through (3) are coupled to the chemical rate equations by equation (8). The chemical rate equations for the reactions

$$\sum_{i=1}^{k} \alpha_{r,i} X_i \underset{k_{b_r}}{\overset{k_{f_r}}{\rightleftarrows}} \sum_{i=1}^{k} \beta_{r,i} X_i \tag{9}$$

can be written as (ref. 8 or 10)

$$\frac{dn_i}{dx} = \frac{1}{\rho u} \sum_r (\beta_{r,i} - \alpha_{r,i})\, k_{f_r} \left[\Pi_i (\rho n_i)^{\alpha_{r,i}} - \frac{1}{K_{c_r}} \Pi_i (\rho n_i)^{\beta_{r,i}} \right] \tag{10}$$

If there are m types of atoms, m of equation (10) can be replaced by statements of conservation of atoms (in this case carbon and oxygen atoms) of the form

$$\sum_{i=1}^{k} a_{z_i} n_i = \sum_{i=1}^{k} a_{z_i} n_{i_s} \tag{11}$$

(which of course can be differentiated to give m values of (dn_i/dx) for use in eq. (8)). The boundary conditions of the flow equations (1), (2), (3), and (8) and the chemical rate equation (10) are specified immediately behind the shock and are at $x = 0$,

$$\rho = \rho_s = \rho_\infty/\epsilon \tag{12}$$

$$u = u_s = \epsilon u_\infty \tag{13}$$

$$p = p_s = \rho_\infty u_\infty^2(1 - \epsilon) \tag{14}$$

$$h = h_s = n_{1_s}(\hat{c}_{p_1} T_s + \hat{h}_1^o) \tag{15a}$$

$$= h_\infty + (1/2)(u_\infty^2 - u_s^2) \tag{15b}$$

$$n_1 = n_{1_s} = (M_1)^{-1}, \quad n_2 = n_3 = n_4 = n_5 = 0 \tag{16}$$

where the strong shock approximation has been used for boundary condition (14), and it has been assumed that the CO_2 does not dissociate in passing through the shock wave in boundary conditions (15) and (16).

A combination of boundary conditions (13) and (15b) with the strong shock approximation (14), and the equation of state (6) yields

$$\epsilon = [2(\hat{c}_{p_1}/\hat{R}) - 1]^{-1} \tag{17}$$

which is needed for the evaluation of the boundary conditions.

Having the set of flow equations and their boundary conditions, we proceed to specify the chemical reactions.

Chemical Reactions

The following reactions are assumed for the dissociation and recombination of CO_2 and its constituents.

$$r = 1, \quad CO_2 + M \rightleftarrows CO + O + M \tag{18}$$

$$r = 2, \quad O_2 + M \rightleftarrows 2O + M \tag{19}^2$$

$$r = 3, \quad CO + M \rightleftarrows C + O + M \tag{20}$$

---

[2]The reactions $r = 2$ turned out to be unimportant in the solutions obtained.

The differential equations can operate on these reactions if the reaction rate coefficients are either known or specified. These coefficients are of the form

$$k_{f_r} = 2[PA\bar{d}^2/\sigma(s-1)!](2\pi\hat{R}T/M^*)^{1/2}(E_{f_r}/\hat{R}T)^{s-1}e^{-(E_{f_r}/\hat{R}T)} \tag{21}$$

or expressed in the Arrhenius form;

$$k_{f_r} = B_{f_r}T^{\alpha_{f_r}}e^{-(E_{f_r}/\hat{R}T)} \tag{22}$$

The backward reaction rate coefficient is included in the equilibrium coefficient

$$K_{c_r} = (k_{f_r}/k_{b_r}) = B_{c_r}T^{\alpha_{c_r}}e^{-(E_{c_r}/\hat{R}T)} \tag{23}$$

This completes the set of equations used to solve the nonequilibrium flow behind the shock wave. It is instructive to have the equilibrium conditions which the nonequilibrium properties eventually approach some distance behind the shock wave.

Equilibrium Conditions

The ten equilibrium properties useful for this analysis are $\bar{n}$, $\bar{n}_1$, $\bar{n}_2$, $\bar{n}_3$, $\bar{n}_4$, $\bar{n}_5$, $\bar{p}$, $\bar{\rho}$, $\bar{T}$, and $\bar{u}$. They are obtained from the simultaneous solution of the following ten algebraic equations. By definition

$$\bar{n} = \bar{n}_1 + \bar{n}_2 + \bar{n}_3 + \bar{n}_4 + \bar{n}_5 \tag{24}$$

Statements of conservation of oxygen and carbon atoms can be expressed as (from eq. (11))

$$\bar{n}_1 + \bar{n}_3 - \bar{n}_5 + \bar{n} = 2n_{1_s} \tag{25}$$

$$\bar{n}_1 + \bar{n}_2 + \bar{n}_5 = n_{1_s} \tag{26}$$

The equation of state is

$$\bar{p} = \bar{\rho}\bar{n}\hat{R}\bar{T} \tag{27}$$

Equilibrium coefficients can be expressed as

$$K_{c_1} = (\bar{n}_2\bar{n}_4/\bar{n}_1)\bar{\rho} = B_{c_1}\bar{T}^{\alpha_{c_1}}\exp(-E_{c_1}/\hat{R}\bar{T}) \tag{28}$$

$$K_{c_2} = (\bar{n}_4^2/\bar{n}_3)\bar{\rho} = B_{c_2}\bar{T}^{\alpha_{c_2}}\exp(-E_{c_2}/\hat{R}\bar{T}) \tag{29}$$

$$K_{c_3} = (\bar{n}_5\bar{n}_4/\bar{n}_2)\bar{\rho} = B_{c_3}\bar{T}^{\alpha_{c_3}}\exp(-E_{c_3}/\hat{R}\bar{T}) \tag{30}$$

and finally the flow relationships

$$\bar{u} = \rho_\infty u_\infty / \bar{\rho} \tag{31}$$

$$\bar{p} = \rho_\infty u_\infty (u_\infty - \bar{u}) \tag{32}$$

and

$$(1/2)(u_\infty^2 - \bar{u}^2) + n_{i_s} \hat{h}_1^{\circ} = \sum_{i=1}^{5} \bar{n}_i (\hat{c}_{p_i} \bar{T} + \hat{h}_i^{\circ}) \tag{33}$$

complete the set of ten simultaneous equations for the ten unknown equilibrium conditions. It is noted that some of the equations are nonlinear and transcendental. These ten algebraic equations were reduced to a set of three nonlinear transcendental equations with $\bar{n}_3$, $\bar{n}_4$, and $\bar{n}_5$ as unknowns and seven equations in the other unknowns. The set of three equations was solved by the oldest of all methods, "regula falsi" (ref. 11). The other seven equations were then solved quite simply for the remaining seven unknowns.

Method of Solution

Solutions of the nonequilibrium flow field were obtained in three ways. These will be referred to as the complete solution, the first approximation, and the second approximation. The two approximate solutions were sought in an effort to obtain as simple a mathematical model as possible. Both approximations are compared with the complete solution to establish their validity.

Complete solution.- Flow equations (1), (2), (3), and (8) were solved simultaneously with the chemical reaction equations (10) and (11) written for the reactions (18), (19), and (20) subject to boundary conditions (12) through (16). The integration was performed by use of the Adams-Moulton predictor-corrector variable step integration scheme (ref. 12). Values for the dissociation energy and some of the other physical constants in the rate coefficients and equilibrium coefficients were either obtained or estimated from information in references 13, 14, 15, and 16. The rate and equilibrium coefficients will be presented subsequently. Computation of one example including both the nonequilibrium flow field and the equilibrium conditions was accomplished in approximately one minute by the IBM 7090 digital computer.

Uncoupling of chemical and flow equations.- An order of magnitude analysis of the flow equations (see appendix) reveals that both p and h can be expected to be almost constant in the flow field. Examination of the flow equations (1), (2), and (3) shows that if any one of the variables p, h, ρ, and u is strictly constant, the other three must be constant. In what will be called the first approximation, we assume that this is the case. Then the flow equations can be omitted and the chemical processes can be studied by use of equations (10), (11), and the equation of state (6). It is noted that T is still a variable because the n_i vary.

Closed form solution.- Another simplification can be effected by what will be referred to as the second approximation. In this case it is assumed that p, h, ρ, and u are constant behind the shock and that only the forward reactions of equations (18) and (20) are important. Furthermore, it is assumed that the forward reaction (18) is essentially completed before the forward reaction (20) begins. That is, the CO_2 is almost completely dissociated before CO begins to dissociate as shown in sketch (b). This assumption will be checked subsequently

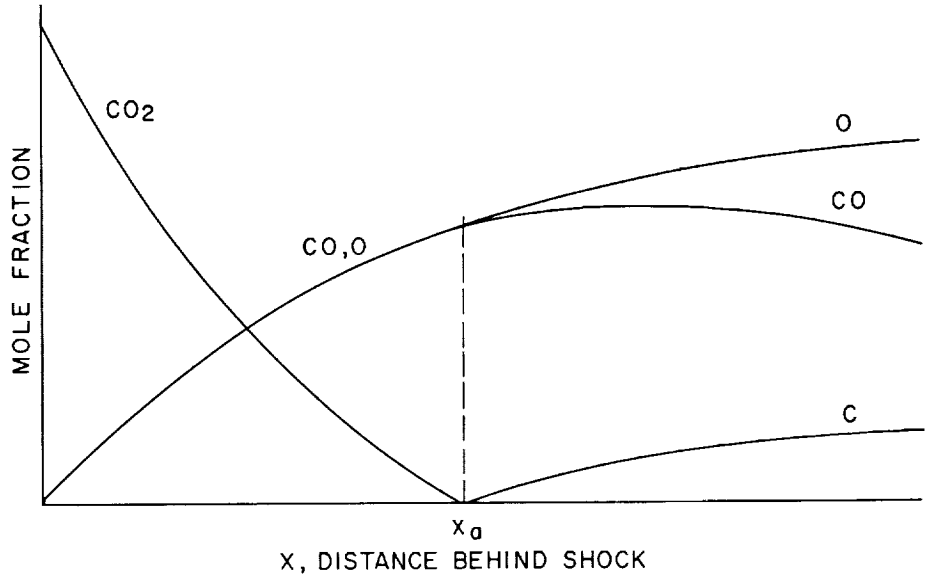

Sketch (b)

by comparison with the results of the complete solution. With these assumptions, the appropriate chemical rate equation (10) and atom conservation equation (11) become, for $x < x_a$,

$$dn_1/dx = -k_{f_1}(\rho/u)_s n_M n_1 \tag{34}$$

$$2n_1 + n_2 + n_4 = 2n_{1_s} \tag{35}$$

$$n_1 + n_2 = n_{1_s} \tag{36}$$

where

$$n_M = n_1 + n_2 + n_4 \tag{37}$$

For $x \geq x_a$,

$$dn_2/dx = -k_{f_3}(\rho/u)_s n_M n_2 \tag{38}$$

$$n_2 + n_4 = 2n_{1s} \tag{39}$$

$$n_2 + n_5 = n_{1s} \tag{40}$$

where

$$n_M = n_2 + n_4 + n_5 \tag{41}$$

Equations (34) through (37) can be combined with the equation of state (6) and the forward rate coefficient equation (22) to yield a first-order differential equation in which n_1 is the only variable,

$$dn_1/dx = -B_{f_1}(p/\rho\hat{R})_s^{\alpha_{f_1}}(\rho/u)_s n_1(2n_{1s} - n_1)^{1-\alpha_{f_1}}\exp[-E_{f_1}(\rho/p)_s(2n_{1s} - n_1)] \tag{42}$$

with the boundary condition, at $x = 0$,

$$n_1 = n_{1s} \tag{43}$$

If $(2n_{1s} - n_1)^{1-\alpha_{f_1}}$ in equation (42) is rewritten

$$(2n_{1s})^{1-\alpha_{f_1}}[1 - (n_1/2n_{1s})]^{1-\alpha_{f_1}}$$

and the latter expression is expanded in a power series, equation (42) can be integrated for $\alpha_{f_1} = 1/2$ with the simple result for $x < x_a$

$$\ln\frac{n_1}{n_{1s}} + a(n_1 - n_{1s}) + \frac{a^2(n_1^2 - n_{1s}^2)}{2\cdot 2!} + \frac{a^3(n_1^3 - n_{1s}^3)}{3\cdot 3!} + \cdots \frac{a^m(n_1^m - n_{1s}^m)}{m\cdot m!} + \cdots$$

$$+ \frac{e^{an_1} - e^{an_{1s}}}{2(2n_{1s}a)} + \frac{3}{2\cdot 4(2n_{1s}a)^2}\left[e^{an_1}(an_1 - 1) - e^{an_{1s}}(an_{1s} - 1)\right]$$

$$+ \frac{3\cdot 5}{2\cdot 4\cdot 6(2n_{1s}a)^3}\left[e^{an_1}(a^2n_1^2 - 2an_1 + 2) - e^{an_{1s}}(a^2n_{1s}^2 - 2an_{1s} + 2)\right]$$

$$+ \frac{3\cdot 5\cdot 7}{2\cdot 4\cdot 6\cdot 8(2n_{1s}a)^4}\left[e^{an_1}(a^3n_1^3 - 3a^2n_1^2 + 6an_1 - 6)\right.$$

$$\left. - e^{an_{1s}}(a^3n_{1s}^3 - 3a^2n_{1s}^2 + 6an_{1s} - 6)\right]$$

$$+ \frac{3\cdot 5\cdot 7\cdot 9}{2\cdot 4\cdot 6\cdot 8\cdot 10(2n_{1s}a)^5}\left[e^{an_1}(a^4n_1^4 - 4a^3n_1^3 + 3a^2n_1^2 - 6an_1 + 6)\right.$$

$$\left. - e^{an_{1s}}(a^4n_{1s}^4 - 4a^3n_{1s}^3 + 3a^2n_{1s}^2 - 6an_{1s} + 6)\right]$$

$$= -B_{f_1}\sqrt{\frac{2n_{1s}p_s}{\rho_s\hat{R}}}\left(\frac{\rho}{u}\right)_s e^{(2n_{1s}a)x} \tag{44}$$

where

$$a = -E_{f_1}\left(\frac{\rho}{p}\right)_s \tag{45}$$

It is noted that x_a is determined where n_1/n_{1_s} is some arbitrarily small value (0.001 for example).

Equations (38) through (41) can be manipulated in the same way to give a differential equation identical to equation (42) with n_1 replaced by n_2, $2n_{1_s}$ replaced by $3n_{1_s}$, and B_{f_1}, α_{f_1}, and E_{f_1} replaced by B_{f_3}, α_{f_3}, and E_{f_3}. Its boundary condition is at $x = x_a$

$$n_2 \approx n_{1_s} \tag{46}.$$

The solution is identical to that shown in equation (44) with the proper interchange of notation; with x replaced by $(x - x_a)$, $(2n_{1_s}a)$ replaced by $(3n_{1_s}a)$ wherever the former appears alone in parentheses, and on the right side of equation (44) $2n_{1_s}$ is replaced by $3n_{1_s}$ under the square root sign.

DISCUSSION OF RESULTS

In presenting results, we first consider reaction rate estimates. Then some typical solutions of the flow equations are shown, and finally relaxation distances are presented.

Reaction Rate Estimates

There are few experimental results for the dissociation rates of CO_2 and CO, especially for the high nonequilibrium temperatures behind normal shock waves. For this reason, it was necessary to estimate forward reaction rates. However, there is no sure way to estimate dissociation rates for diatomic molecules, and estimates for triatomic molecules are even more uncertain. The principal uncertainties are the values of s (the number of classical squared terms of energy contributing to the reaction), P (the steric factor or transition probability), and E_{f_r} (the activation energy). The lower limit of s and the upper limit of P are unity. The simplest first estimate is made with these limiting values of s and P and with the dissociation energy for the activation energy. This approximation is equivalent to the assumption that the colliding pairs must have translational energy greater than or equal to the dissociation energy if a reaction is to occur, and that a collision of any such pair always results in a reaction. The corresponding rate coefficient estimates for CO_2 and CO dissociation are shown as solid lines in figure 1.

Although, in fact, s is greater than unity and P is less than unity, it can be shown by the following discussion that for reasonable values of each, the

effects tend to cancel one another and the simple estimate used here is plausible. The upper limit of s for the collision of a CO_2 molecule with an atom is 6. The limit is higher for collision with another molecule. Similarly, the upper limit of s for collision of CO with an atom is either 2 or 3, and for collision with a diatomic molecule is either 3 or 5. If we assume for illustrative purposes that $s = 5$ for CO_2 dissociation and 3 for CO dissociation, while P is unity, the reaction rate coefficients for these two reactions are shown by dashed lines in figure 1. At temperatures below 20,000° K, they are higher than the corresponding solid lines by a factor of the order of 10 to 10^3. However, if P were of the order of 10^{-1} to 10^{-3}, the effect would be canceled and we would come back to about the same estimate obtained for $s = P = 1$. Examination of rate data for oxygen dissociation indicates that P is probably of the order of 10^{-2} for that reaction. Thus we conclude that the simple first estimate using $P = s = 1$ leads to plausible rate coefficients in the temperature range up to 20,000° K. At temperatures greater than 20,000° K, the rates for $s > 1$ and $P = 1$ differ from the estimates for $s = P = 1$ by less than a factor of 10. Thus since s is probably greater than 1, while P is much less than 1, the rates predicted by setting $s = P = 1$ are expected to be high. Because of the preceding argument, it is speculated that relaxation phenomena may be even slower and relaxation distances may be even larger than the results of the present estimates will show.

Experimental results for the reaction

$$CO_2 + A \rightarrow \text{products} \tag{47}$$

have been obtained (by Brabbs, Belles, and Zlatarich) at temperatures to about 3000° K, from which the reaction rate coefficient

$$k_f = 3\times10^{11}T^{1/2}\exp(-86/\hat{R}T)\,\text{cm}^3\text{mole}^{-1}\text{sec}^{-1} \tag{48}$$

was obtained, which is also shown in figure 1. It is noted that the curve corresponding to equation (48) is in fair agreement with the present estimate for CO_2 dissociation in the temperature range 5,000° K to 10,000° K.

The curve for oxygen dissociation shown in figure 1 was obtained from reference 15 (in which the results of ref. 16 were extrapolated to temperatures in excess of 20,000° K).

Equilibrium coefficients for the three reactions considered are shown in figure 2. These were obtained by an empirical fit of equation (23) to the numerical results of references 12 and 13.

A summary of the constants used in the forward reaction rate coefficients and equilibrium coefficients is shown in the following table.

Reaction summary						
r	B_{f_r}, $\frac{cm^3}{g\ mol\ sec\ {}^{o}K^{\alpha_{f_r}}}$	α_{f_r}	E_{f_r}, $\frac{k\ cal}{g\ mol}$	B_{c_r}, $\frac{g\ mol}{cm^3\ {}^{o}K^{\alpha_{c_r}}}$	α_{c_r}	E_{c_r}, $\frac{k\ cal}{g\ mol}$
1	6.955×10^{12}	0.5	125.7497	0.50596×10^{14}	-2.9713	138.7454
2	11.9×10^{20}	-1.5	117.9982	$.33399\times10^{4}$	-.6038	119.4466
3	7.7206×10^{12}	.5	256.1742	$.34113\times10^{3}$	-.2366	257.4958

Solutions

Before a few typical solutions are examined, it is instructive to examine the equilibrium values which the flow-field properties approach asymptotically some distance behind the shock. Both static enthalpy and pressure are almost constant behind the shock (see appendix). Thus we can expect that $\bar{p}/p_s$ and $\bar{h}/h_s$ are approximately unity. Indeed, for flight speeds between 5 and 10 km/sec in CO_2 at ambient density between 10^{-2} and 10^{-4}, standard atmospheric density $\bar{p}/p_s$ and $\bar{h}/h_s$ differed from unity by less than 3 percent. First, estimates of $\bar{p}$ and $\bar{h}$ can thus be obtained from equations (14) and (15b) directly. However, $\bar{\rho}$ and $\bar{T}$, shown in figures 3 and 4, are quite different from ρ_s and T_s. It is seen that $\bar{\rho}$ is not a strong function of shock speed. Moreover, $\rho_\infty/\bar{\rho}$ varies between the narrow limits 0.0472 to 0.0628 for the entire range of conditions mentioned previously. Equilibrium temperatures shown in figure 4 are fairly strong functions of both shock speed and ambient density.

Turning now to the solutions of the chemical rate and flow equations, we examine first a case of a shock moving at fairly high speed (9 km/sec) into CO_2 at low density ($\rho_\infty/\rho_o = 10^{-4}$). Flow-field quantities are shown in figure 5(a) and chemical species concentrations are shown in 5(b). Note that quite large variations in the flow-field quantities u, ρ, and T occur because of the chemical relaxation processes.

It is interesting to observe that behind the shock, the flow accelerates and then decelerates because of the chemical relaxation processes. Correspondingly, density diminishes and then increases so that the product of density and velocity remains constant (eq. (1)). Generally, at lower shock speeds in air, density increases monotonically in the dissociative relaxation region behind the shock (ref. 17). For that reason, the negative density gradient behind the shock in CO_2 may be a little surprising.

The conditions for which the density gradient behind the shock is positive or negative can be derived as follows. Just behind the shock, $n_2 = n_3 = n_4 = n_5 = 0$ and $dn_3/dx = dn_5/dx = 0$ (because there is no atomic oxygen to recombine and there is no carbon monoxide to dissociate). Using this information with the equation of state (6), boundary conditions (12), (13), (14), equations (17), (11), and

(8) leads to

$$\left(\frac{du}{dx}\right)_s \approx \frac{u_s}{n_{1_s}(\hat{c}_{p_1}/\hat{R})}\left(\frac{dn_1}{dx}\right)_s \left\{ -2\,\frac{\hat{c}_{p_1}}{\hat{R}} + \frac{\hat{c}_{p_2}}{\hat{R}} + \frac{\hat{c}_{p_4}}{\hat{R}} + \frac{-\hat{h}_1^{\circ} + \hat{h}_2^{\circ} + \hat{h}_4^{\circ}}{\frac{u_\infty^2}{n_{1_s}}\,\frac{2(\hat{c}_{p_1}/\hat{R} - 1)}{[2(\hat{c}_{p_1}/\hat{R}) - 1]^2}} \right\} \tag{49}$$

As long as CO_2 is dissociating behind the shock, $(dn_1/dx)_s$ is negative. Then $(du/dx)_s$ is $\mp$ or $(d\rho/dx)_s$ is $\pm$ if the braces in equation (49) are $\pm$. Rearranging the quantities in the braces and substituting numerical values for $\hat{h}_1^{\circ}$ and n_{1_s} leads to the criteria

$$\left(\frac{d\rho}{dx}\right)_s \gtrless 0 \text{ if } u_\infty^2 \lessgtr \frac{5.98\times10^{10}\left(2\,\frac{\hat{c}_{p_1}}{\hat{R}} - 1\right)^2}{\left(\frac{\hat{c}_{p_1}}{\hat{R}} - 1\right)\left(2\,\frac{\hat{c}_{p_1}}{\hat{R}} - \frac{\hat{c}_{p_2}}{\hat{R}} - \frac{\hat{c}_{p_4}}{\hat{R}}\right)} \text{ cm}^2/\text{sec}^2 \tag{50}$$

Applying equation (50) to the case where all species are fully excited leads to the approximate result $(d\rho/dx)_s \gtrless 0$ if $u_\infty \lessgtr 5$ km/sec. For no vibrational excitation, the 5 is changed to about 9 km/sec.

In figure 5, the solid lines correspond to the complete solution of the coupled chemical and flow equations. The long dashed lines correspond to the first approximation in which the chemistry and flow are uncoupled and only the chemical rate equations are solved. The short dashed lines correspond to the closed-form solution of the second approximation in which only the forward reactions are considered. For this flight condition, neither approximation represents the temperature or concentration profiles of the complete solution very well. Evidently the coupling between the flow field and the chemical rate processes is important; and, as can be seen in figure 5(b), CO_2 is not completely dissociated before CO begins to dissociate, contrary to the assumption made in the second approximation. It is particularly noteworthy in figure 5(a) that the flow field is still far from equilibrium 10 centimeters behind the shock.

It is interesting to observe the effect of a large change in reaction rate. In figures 6(a) and 6(b), the solid lines correspond to the complete solution shown previously in figure 5. The dashed lines are the result of changing s in reactions (18) and (20) to 5 and 3, respectively, leaving P fixed at unity. This corresponds loosely to increasing the reaction rates by about two or three orders of magnitude. It is seen that equilibrium is approached more rapidly for the latter condition (although relaxation distance is only changed about one order of magnitude) as would be expected. However, for the reasons mentioned previously, the solid lines are believed to be a more realistic representation of the flow field.

Figures 7(a) and 7(b) show flow-field and concentration profiles for a lower flight speed at the same ambient density. Here the first and second approximations give almost identical results and both are a reasonable representation of the temperature and concentration profiles of the complete solution. The results indicate that only reaction (18) was of any consequence at this speed.

A result of high-speed flight (u_∞ = 10 km/sec) at one hundred times higher density ($\rho_\infty/\rho_O = 10^{-2}$) is shown in figures 8(a) and 8(b). Again for high speed, neither approximation represents the complete solution very well. Here it is noted that most of the chemical relaxation has taken place in a distance of 0.1 cm behind the shock.

In figures 9(a) and 9(b), the flow field is that of a low shock speed at a high ambient density. Here again, the dissociation of CO_2 was the only significant reaction, as may be expected.[3] Both approximations were reasonable representations of the flow field.

Comparison of CO_2 With Other Gases

For strong shock waves, the flow behind the shock can be characterized by two free-stream variables, velocity and ambient density. For a fixed free-stream velocity and ambient density, we will compare results in CO_2 with those in air, nitrogen, and oxygen.

Insofar as equilibrium conditions behind shock waves are concerned, the pressure is very nearly the same for all of these gases. However, considerably lower equilibrium temperature, density, and mole fraction of ions or electrons exist behind high-speed shock waves in CO_2 than in air.

With regard to nonequilibrium processes, it is pointed out that in terms of dissociation energy, CO_2 is more stable than O_2 but less stable than N_2. Also, CO is more stable than N_2. Thus for high-speed shock waves for which both CO_2 and the resulting CO dissociate, we would expect relaxation to proceed more slowly in CO_2 than in O_2, N_2, or air. Conversely, for low-speed shock waves behind which CO_2 dissociates but CO does not, we would expect relaxation to proceed more rapidly in CO_2 than in N_2.

The nonequilibrium flow-field profiles behind shocks moving at 9 km/sec at ambient density $\rho_\infty/\rho_O = 10^{-4}$ in pure CO_2 and pure N_2 are compared in figure 10. Reaction rates for N_2 dissociation were obtained from reference 18. Relaxation in CO_2 is slower than in N_2, as was expected. The initial dip in the density profile appears to be missing in the N_2 flow. It is actually there, however, but is small and almost at the origin.

A comparison of CO_2 with N_2 and O_2 can be summarized in terms of the degree of completion η (which is defined subsequently) of the chemical relaxation. That is, at a distance of 10 centimeters behind the shock wave (again

---

[3]In figure 9(b), the concentration of O is slightly less than that of CO because some of the atomic oxygen recombined to form a trace of O_2.

U_∞ = 9 km/sec, $\rho_\infty/\rho_o = 10^{-4}$), the chemical relaxation is about 60 percent complete in CO_2, but is about 85 percent complete in N_2, while at a distance of only 0.05 cm behind the shock in O_2, the chemical relaxation is 99 percent complete.

The above results will be summarized in a general way subsequently. Before drawing our conclusions, however, it is worthwhile to examine the results of numerous solutions from the standpoint of relaxation distances.

Relaxation Distances

For the present purposes, the relaxation distance is defined as the distance behind the shock at which the change in number of moles that has occurred is a specified fraction of the total change necessary to achieve equilibrium. That is, the relaxation distance is that distance behind the shock at which

$$\eta = \frac{\sum_{i=1}^{k} n_i - n_{1_s}}{\sum_{i=1}^{k} \bar{n}_i - n_{1_s}} \tag{51}$$

where η is a specified value less than unity. Thus η is an index of how far the chemical reactions have gone toward completion. Figures 11 through 14 are contour charts of relaxation distance as a function of shock speed and ambient density for η = 0.1, 0.5, 0.8, and 0.95, respectively. It can be seen that the relaxation distance for 10-percent reaction completion is small, varying from 10^{-5} to 10^{-2} cm as ρ_∞/ρ_o varies from 10^{-1} to 10^{-4}. On the other hand, relaxation distances for 95-percent completion can be large, varying from 10^{-1} to 10^{3} cm as ρ_∞/ρ_o varies from 10^{-1} to 10^{-4}.

CONCLUDING REMARKS

A study was made of the dissociative relaxation of carbon dioxide and its components behind normal shock waves moving at speeds between 5 and 10 km/sec at ambient densities from 10^{-2} to 10^{-4} times standard atmospheric density. Because of a lack of high-temperature chemical reaction-rate data, it was necessary to use collision theory for estimating rate processes. The analysis was simplified somewhat and it was assumed that vibrational relaxation could be neglected. It was also assumed that the specific heat of a pure species was constant at its classical fully excited value. The latter assumption is quite reasonable for single particle species C and O in the regime of the analysis, but less valid for the species CO and CO_2. Certainly when more is known of reaction rates, it would be appropriate to refine the other assumptions used in the study.

The dissociation and recombination reactions for CO_2, O_2, and CO were considered, in the analysis, and the results indicated that the dissociation and recombination of O_2 could have been neglected. The analysis results also showed that at large distances behind the shock for shock speeds of about 6 km/sec, CO_2

was almost completely dissociated but CO did not dissociate. On the other hand, at shock speeds of 10 km/sec almost everything was dissociated and the end products consisted principally of atomic carbon and oxygen. It should be noted, however, that ionizing reactions were not considered in the analysis and that, at 10 km/sec, some ionization may be present.

Strong coupling was indicated between the chemical relaxation and the flow field in the nonequilibrium part of the flow. The coupling effects were strong for high-speed shocks regardless of density level. The coupling for high-speed shocks causes density to first decrease and then increase toward the equilibrium value. Particle velocity behaves in the reverse way. A simple criterion was developed to show conditions for which the density gradient behind the shock wave is positive or negative.

Two approximations were employed to obtain solutions. The first of these uncoupled the chemical effects from the flow field. The second, which uncoupled the chemical effects and in addition considered only the dissociation reactions, led to a closed-form solution. Both approximations take into account the varying temperature in the relaxation region. Comparison of the results with those of the complete solutions indicated that both approximations gave about the same result for temperature and concentration profiles at shock speeds up to 6 km/sec and both were a reasonable representation of the complete solution. At shock speeds of 10 km/sec, however, neither approximation represented the complete solution very well.

Results show that flow fields behind high-speed shock waves are farther from chemical equilibrium in CO_2 than in N_2 or O_2.

Finally, relaxation distances behind the shock were large for low density. For ambient density of the order of 10^{-4} standard density, the relaxation distance for reactions to go 95 percent toward completion was of the order of 10 meters.

Ames Research Center
National Aeronautics and Space Administration
Moffett Field, Calif., March 19, 1963

18

APPENDIX

ORDER OF MAGNITUDE DISCUSSION

In the strict sense, all of the flow-field quantities ρ, u, p, h, T and species concentration vary in the reacting flow field behind the shock. Some of these quantities, however, will vary more than others. The purpose of the following discussion is to show the relative variation of the quantities ρ, u, p, and h in the flow field behind the shock.

At some distance x behind the shock, the ratio of local density to the density immediately behind the shock is defined as g.

$$\frac{\rho}{\rho_s} \equiv g \tag{A1}$$

Thus the change in ρ from ρ_s is

$$\frac{\rho - \rho_s}{\rho_s} = \frac{\Delta\rho}{\rho_s} = g - 1 \tag{A2}$$

The corresponding change in u is from equation (1)

$$\frac{\Delta u}{u_s} = \frac{1}{g} - 1 \tag{A3}$$

Similarly, from equation (2) the change in p (noting that $p_s \approx \rho_\infty u_\infty^2 = \rho_s u_s u_\infty$) is

$$\frac{\Delta p}{p_s} = \epsilon \left(1 - \frac{1}{g}\right) \tag{A4}$$

where $\epsilon = \rho_\infty/\rho_s$. Finally, the change in h if we assume that $h_\infty \ll h_s$ and $u_\infty^2 \gg u_s$ and make use of the integrated form of equation (3) is approximately

$$\frac{\Delta h}{h_s} = \epsilon^2 \left(1 - \frac{1}{g^2}\right) \tag{A5}$$

Assuming for exemplary purposes that g may be as high as 2, and that $\epsilon \approx 10^{-1}$, the corresponding changes in density, velocity, pressure, and enthalpy (from eqs. (A2) through (A5)) are 100, 50, 5, and 0.75 percent, respectively. Similarly, if g is as small as 1/2, we arrive at the same qualitative result. Thus we conclude that pressure and enthalpy do not vary greatly in the chemical relaxation region, although density and particle velocity vary a great deal.

REFERENCES

1. Howe, J. T., and Viegas, J. R.: The Dissociative Relaxation of CO_2 Behind Normal Shock Waves. Paper presented at AAS Interplanetary Missions Conference, Los Angeles, 1963.

2. Kaplan, Lewis D.: A Preliminary Model of the Venus Atmosphere. Tech. Rep. 32-379, Jet Propulsion Lab., Pasadena, Calif., Dec. 12, 1962.

3. Yee, Layton, Bailey, Harry E., and Woodward, Henry T.: Ballistic Range Measurements of Stagnation-Point Heat Transfer in Air and in Carbon Dioxide at Velocities up to 18,000 Feet per Second. NASA TN D-777, 1961.

4. Thomas, M.: The High Temperature Transport Properties of Carbon Dioxide, Rep. SM-37790, Douglas Aircraft Co., 1960.

5. Hoshizaki, H.: Heat Transfer in Planetary Atmospheres at Super Satellite Speeds. ARS Jour., Oct. 1962, pp. 1544-1551.

6. Woodward, Henry T.: Thermodynamic Properties of Carbon-Dioxide and Nitrogen Mixtures Behind a Normal Shock Wave. NASA TN D-1553, 1963.

7. Gaydon, A. G., and Hurle, I. R.: Measurement of Times of Vibrational Relaxation and Dissociation Behind Shock Waves in N_2, O_2, Air, CO, CO_2, and H_2. Eighth Symposium (International) on Combustion, Williams and Wilkins, 1962.

8. Vincenti, W. G.: Calculations of the One Dimensional Nonequilibrium Flow of Air Through a Hypersonic Nozzle. Stanford University Department of Aeronautical Engineering Interim Report to AEDC, May 1961.

9. Wilson, A. H.: Thermodynamics and Statistical Mechanics. Cambridge University Press, 1957, p. 136.

10. Penner, S. S.: Chemical Reactions in Flow Systems. Butterworths Scientific Pub., London, Agardograph 7, 1955.

11. Scarborough, J. B.: Numerical Mathematical Analysis. Johns Hopkins Press, 1958, p. 187.

12. Hildebrand, F. B.: Introduction to Numerical Analysis. McGraw-Hill Book Co., 1956.

13. Raymond, J. L.: Thermodynamic Properties of Carbon Dioxide to 24,000° K with Possible Application to the Atmosphere of Venus. Rand Corp. RM-2292, Nov. 1958.

14. Gilmore, F. R.: Properties of Air to 24,000° K. Rand Corp. RM-1543, 1955, or ASTIA Doc. AD-84052.

15. Choudhury, P. R.: An Order of Magnitude Study of the Chemical State of the Shock Layer at the Stagnation Region of a Spherical Body Traveling at Hypersonic Speed. Western States Section of the Combustion Institute, Second Conference on Kinetics, Equilibria and Performance of High Temperature Systems, April 1962.

16. Eschenroeder, A. Q., Boyer, D. W., and Hall, G. T.: Exact Solutions for Nonequilibrium Expansions of Air with Coupled Chemical Reactions. Cornell Aeronautical Laboratories Rep. A.F. 1413-A-1, May 1961.

17. Duff, R. E.: Calculation of Reaction Profiles Behind Steady State Shock Waves. II The Dissociation of Air. Jour. Chem. Phys., vol. 31, no. 4, Oct. 1959.

18. Bortner, M. H., and Golden, J. A.: A Critique on Reaction Rate Constants Involved in the Chemical System of High Temperature Air. General Electric Rep. R61SD023, 1961.

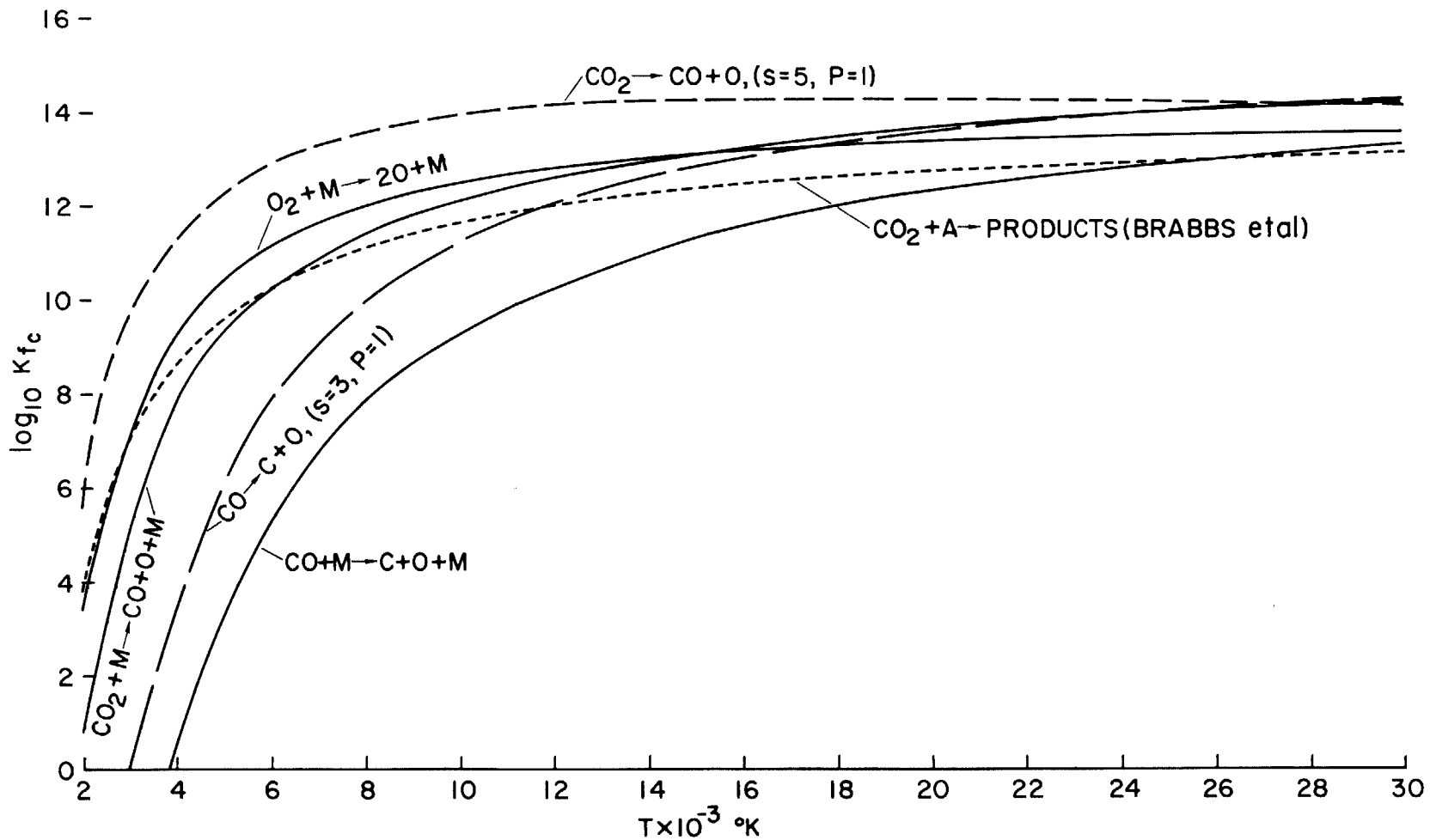

Figure 1.- Forward reaction rate coefficients.

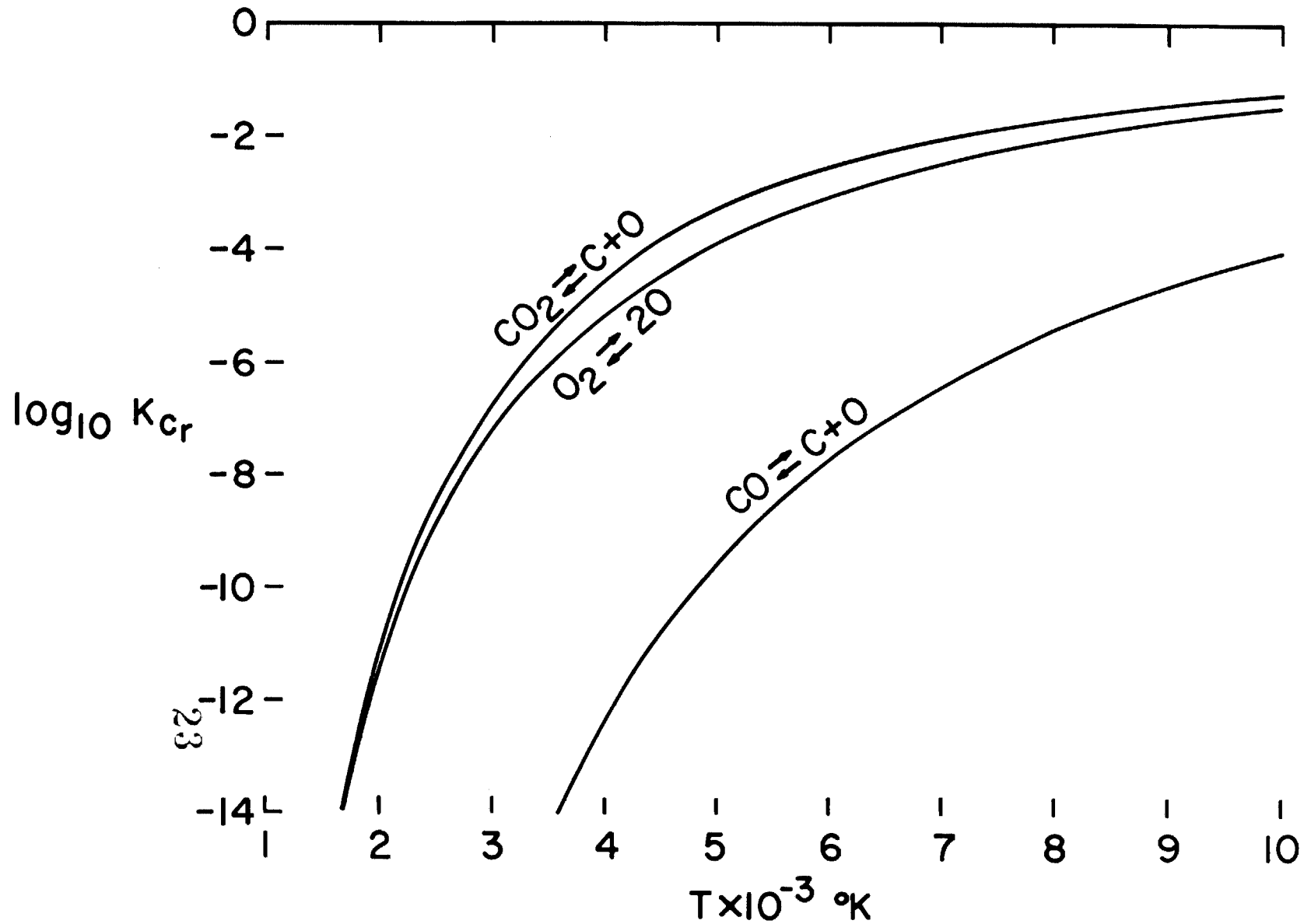

Figure 2.- Equilibrium coefficients.

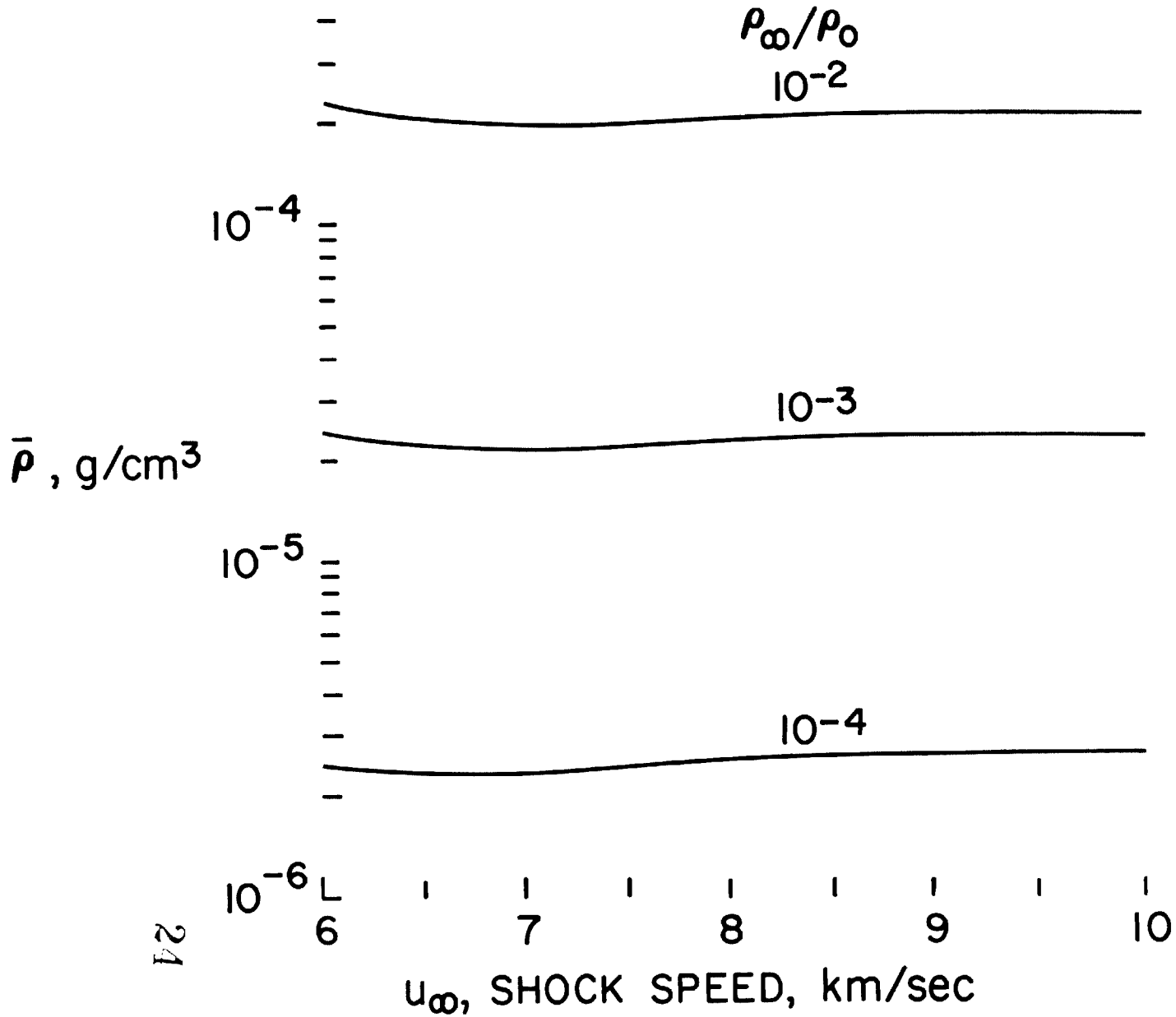

Figure 3.- Equilibrium values of density behind normal shock.

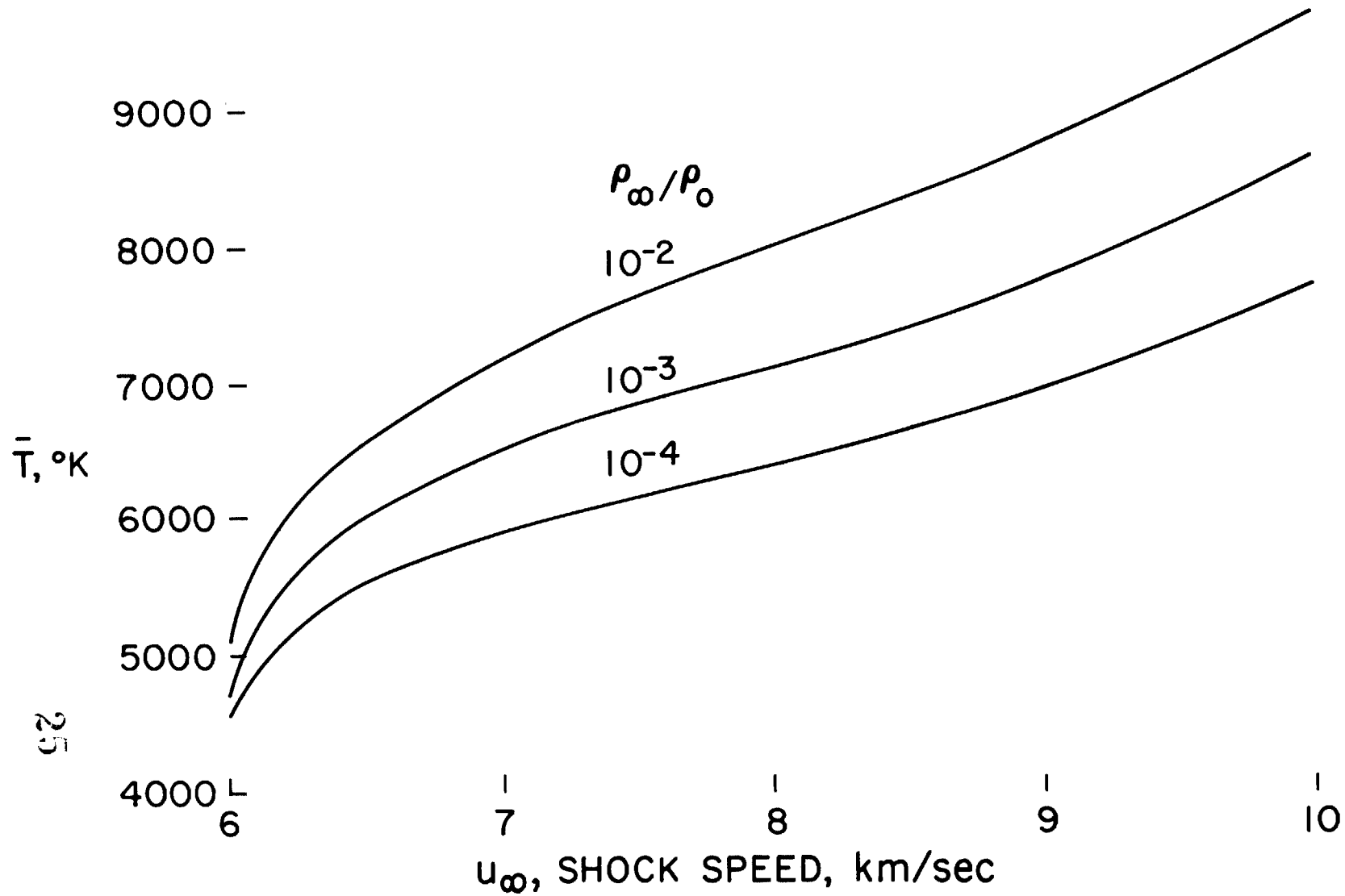

Figure 4.- Equilibrium values of temperature behind normal shock.

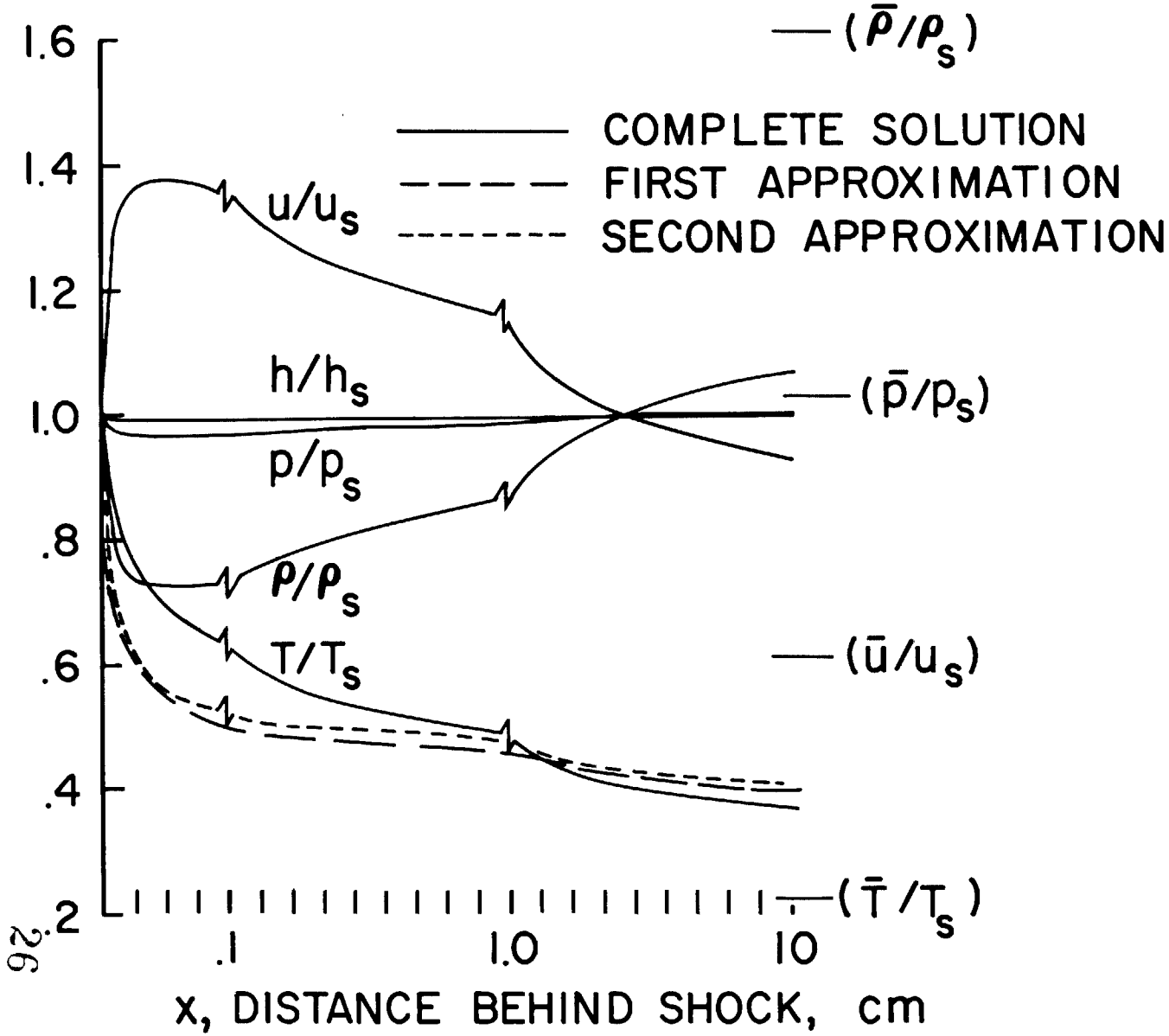

(a) Velocity and thermodynamic properties.

Figure 5.- Nonequilibrium flow-field profiles (u_∞ = 9 km/sec, $\rho_\infty/\rho_O = 10^{-4}$).

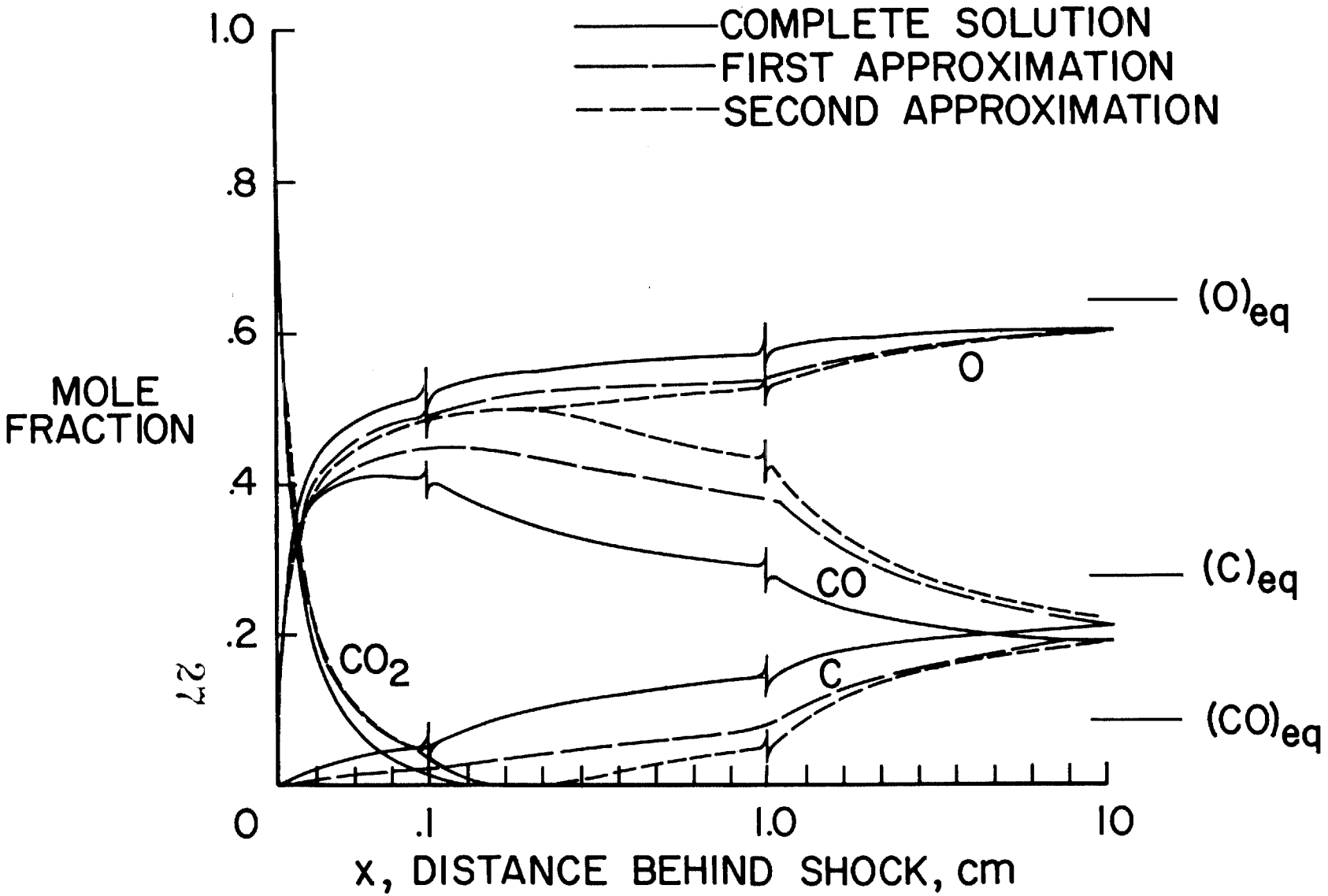

(b) Species concentration.

Figure 5.- Concluded.

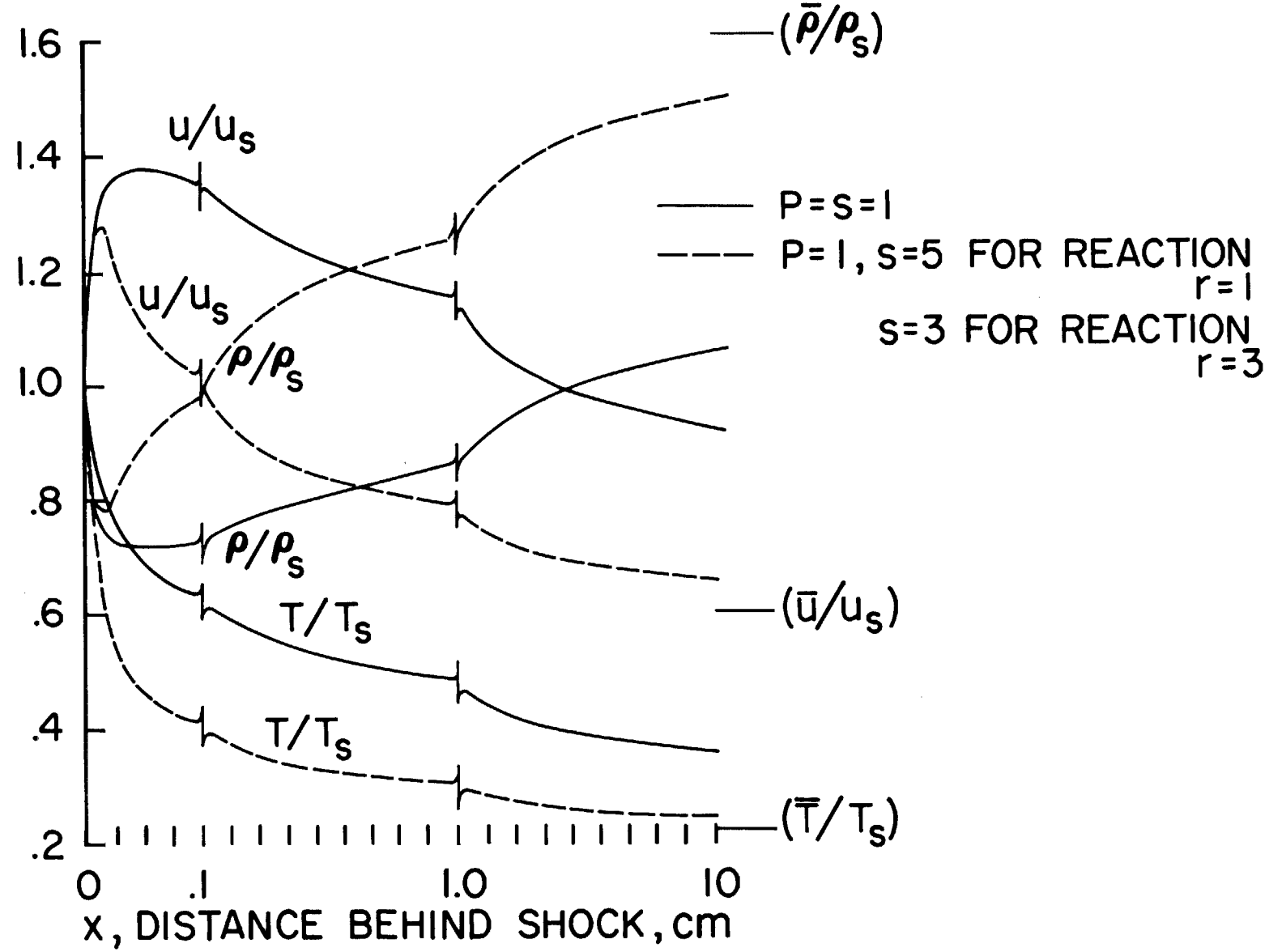

(a) Flow-field profiles (u_∞ = 9 km/sec, $\rho_\infty/\rho_o = 10^{-4}$).

Figure 6.- Effect of large change in reaction rate.

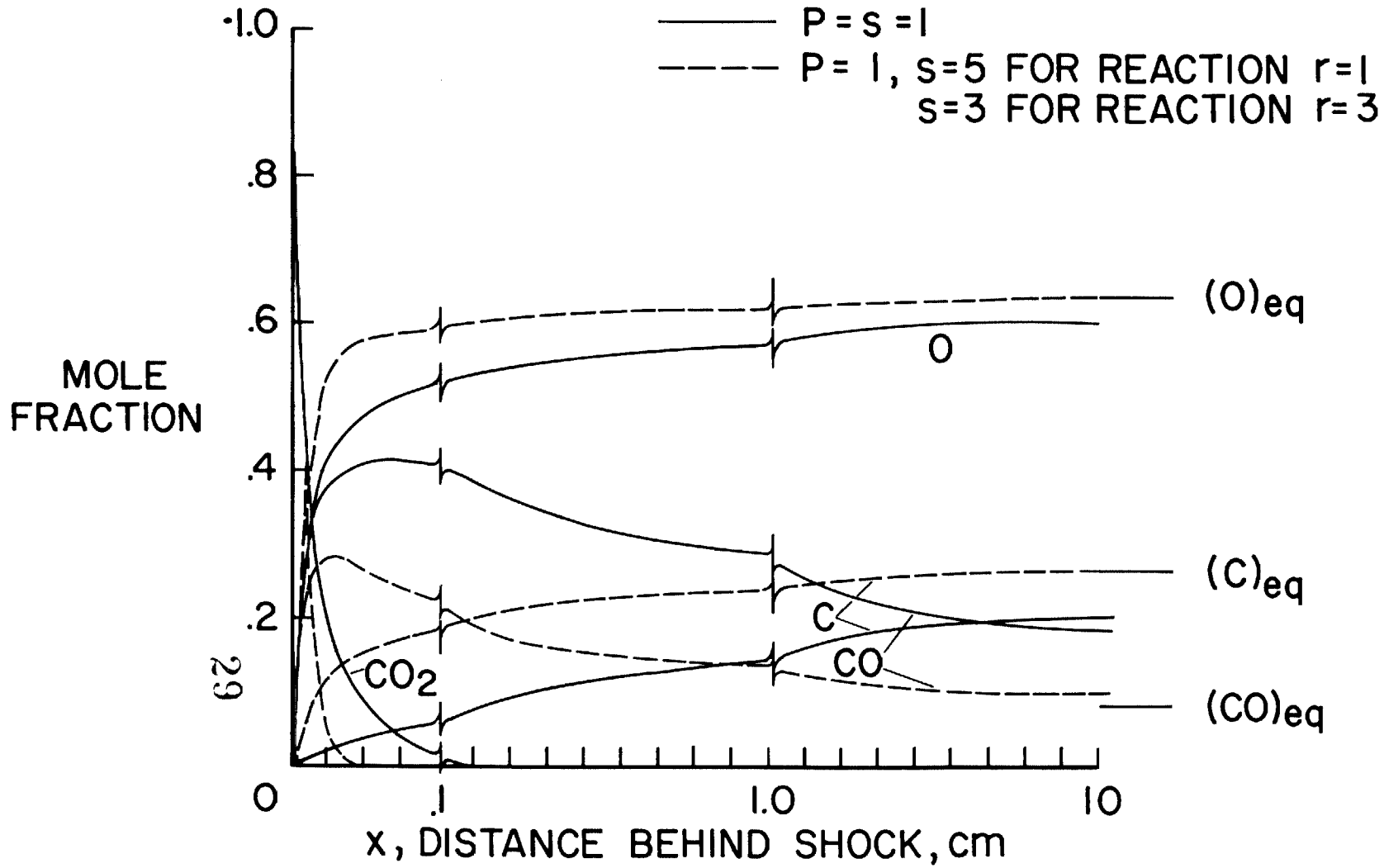

(b) Concentration profiles (u_∞ = 9 km/sec, $\rho_\infty/\rho_o = 10^{-4}$).

Figure 6.- Concluded.

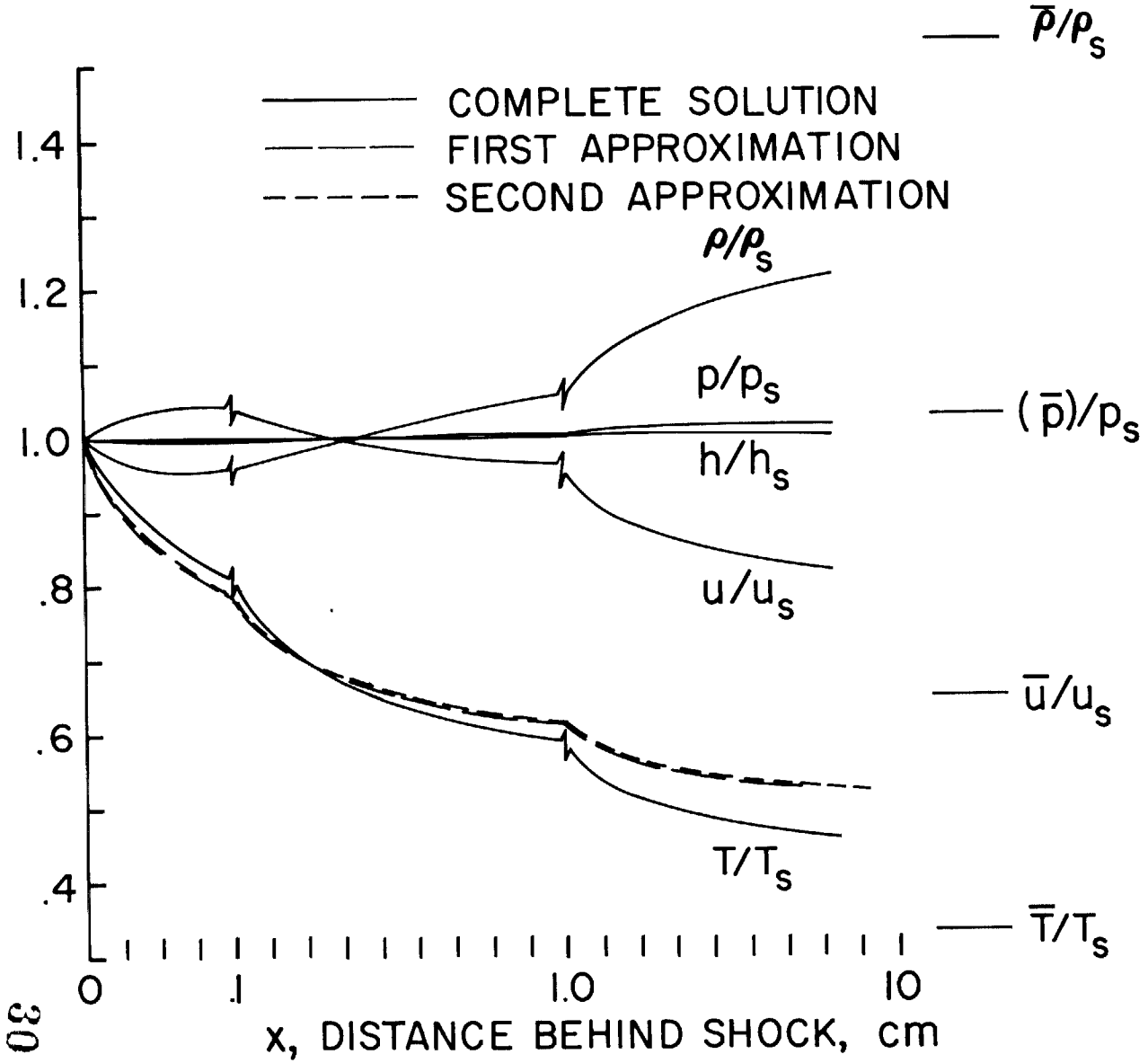

(a) Velocity and thermodynamic properties.

Figure 7.- Nonequilibrium flow-field profiles (u_∞ = 6 km/sec, $\rho_\infty/\rho_o = 10^{-4}$).

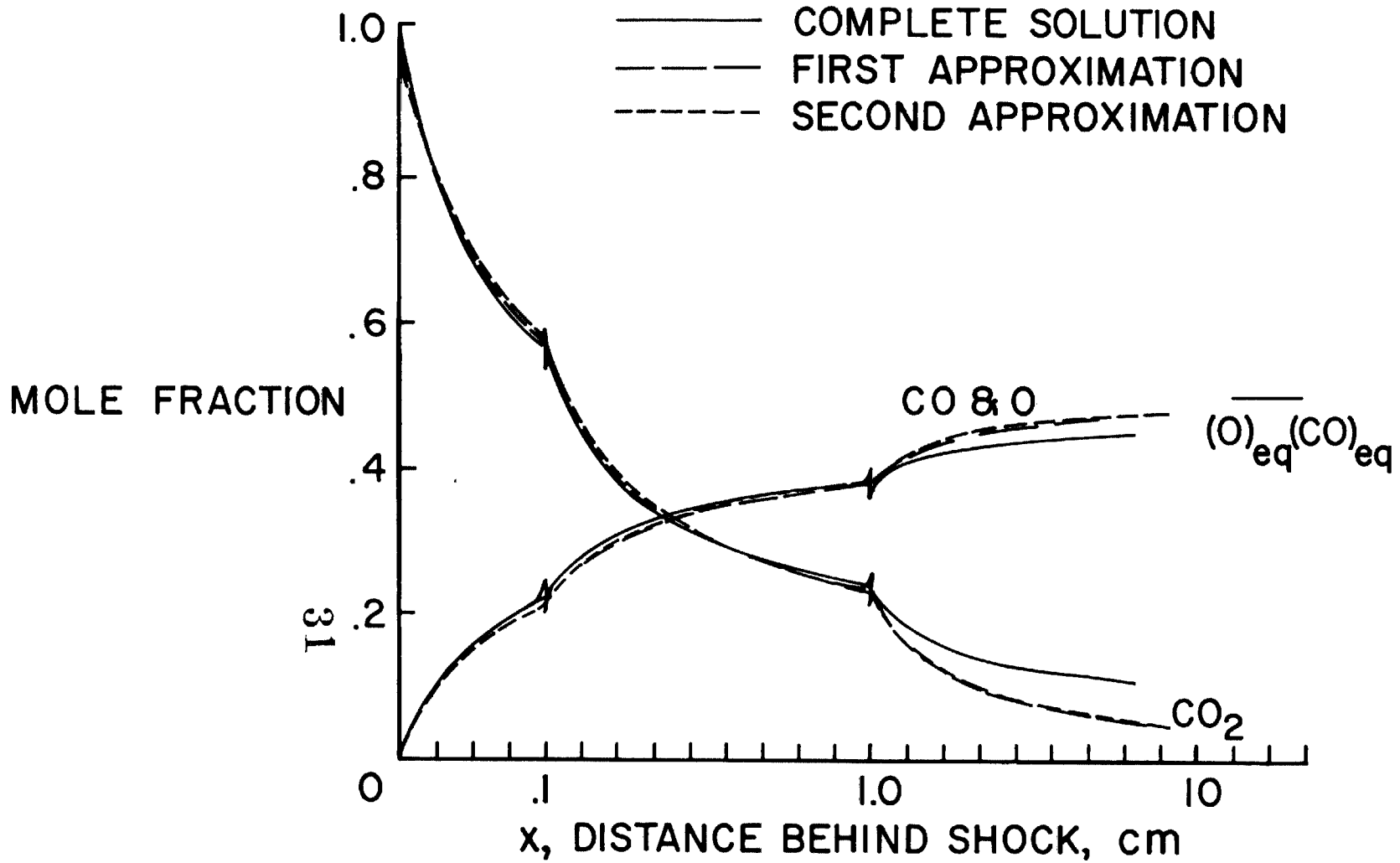

(b) Species concentration.

Figure 7.- Concluded.

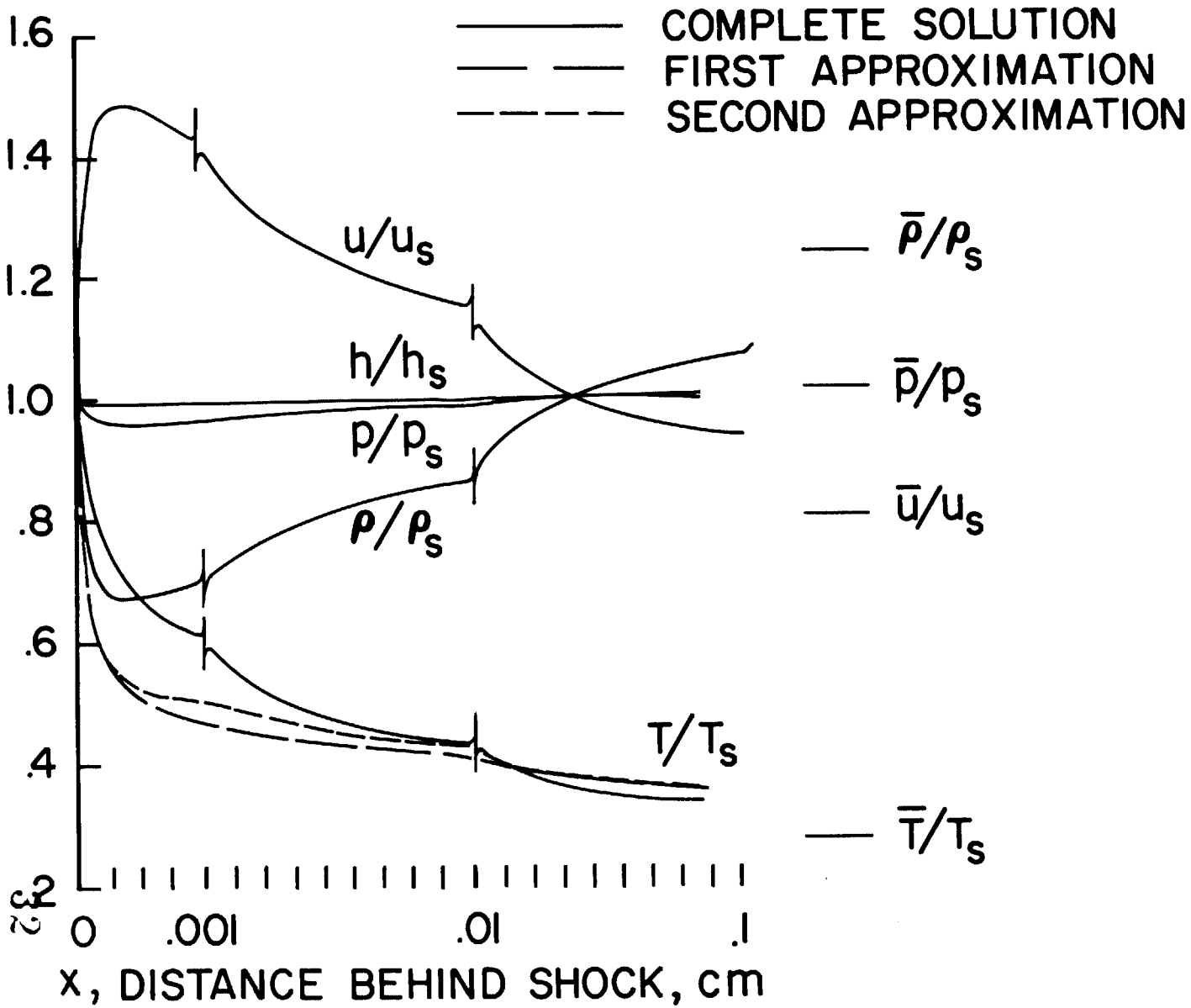

(a) Velocity and thermodynamic properties.

Figure 8.- Nonequilibrium flow-field profiles (u_∞ = 10 km/sec, $\rho_\infty/\rho_O = 10^{-2}$).

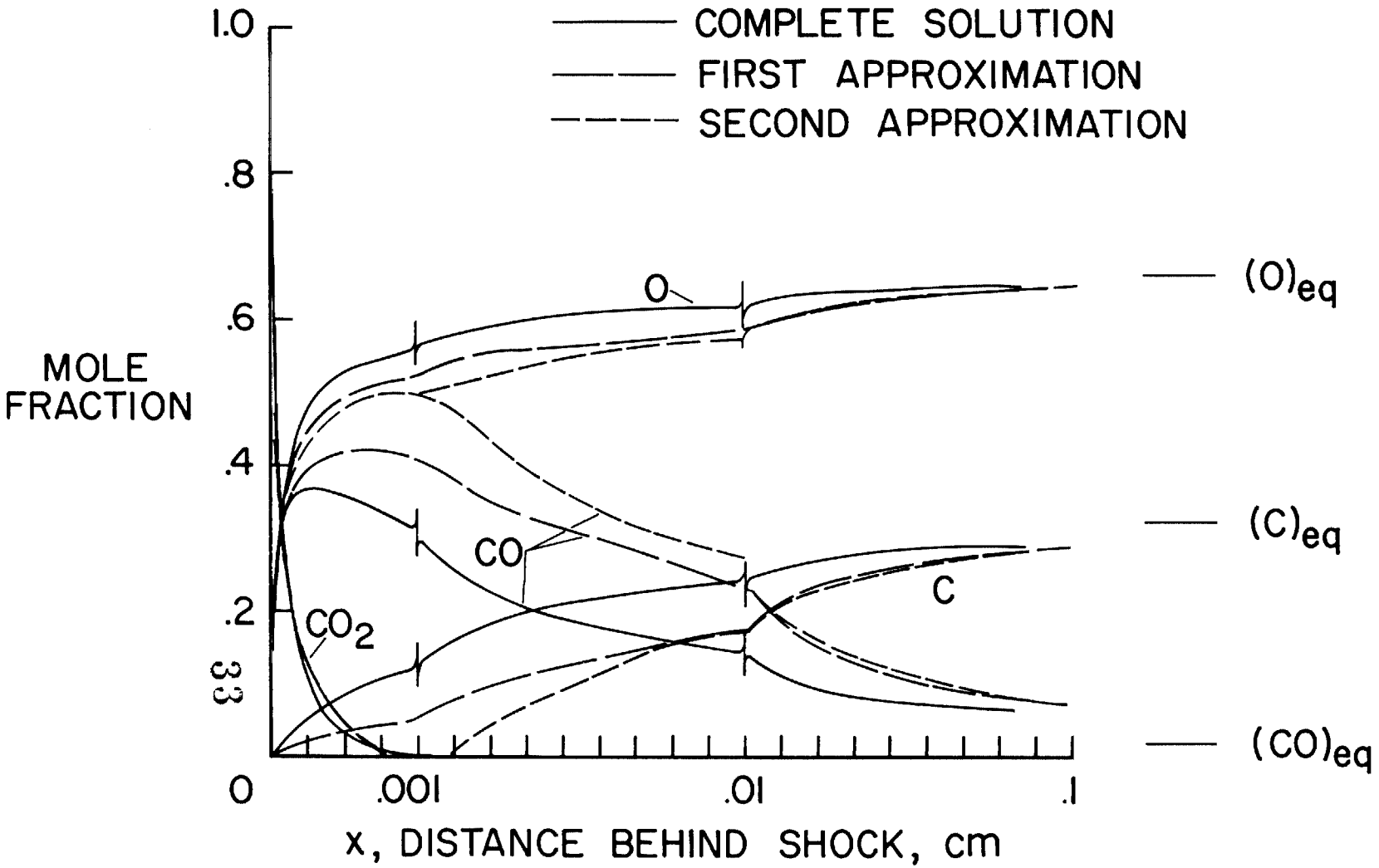

(b) Species concentration.

Figure 8.- Concluded.

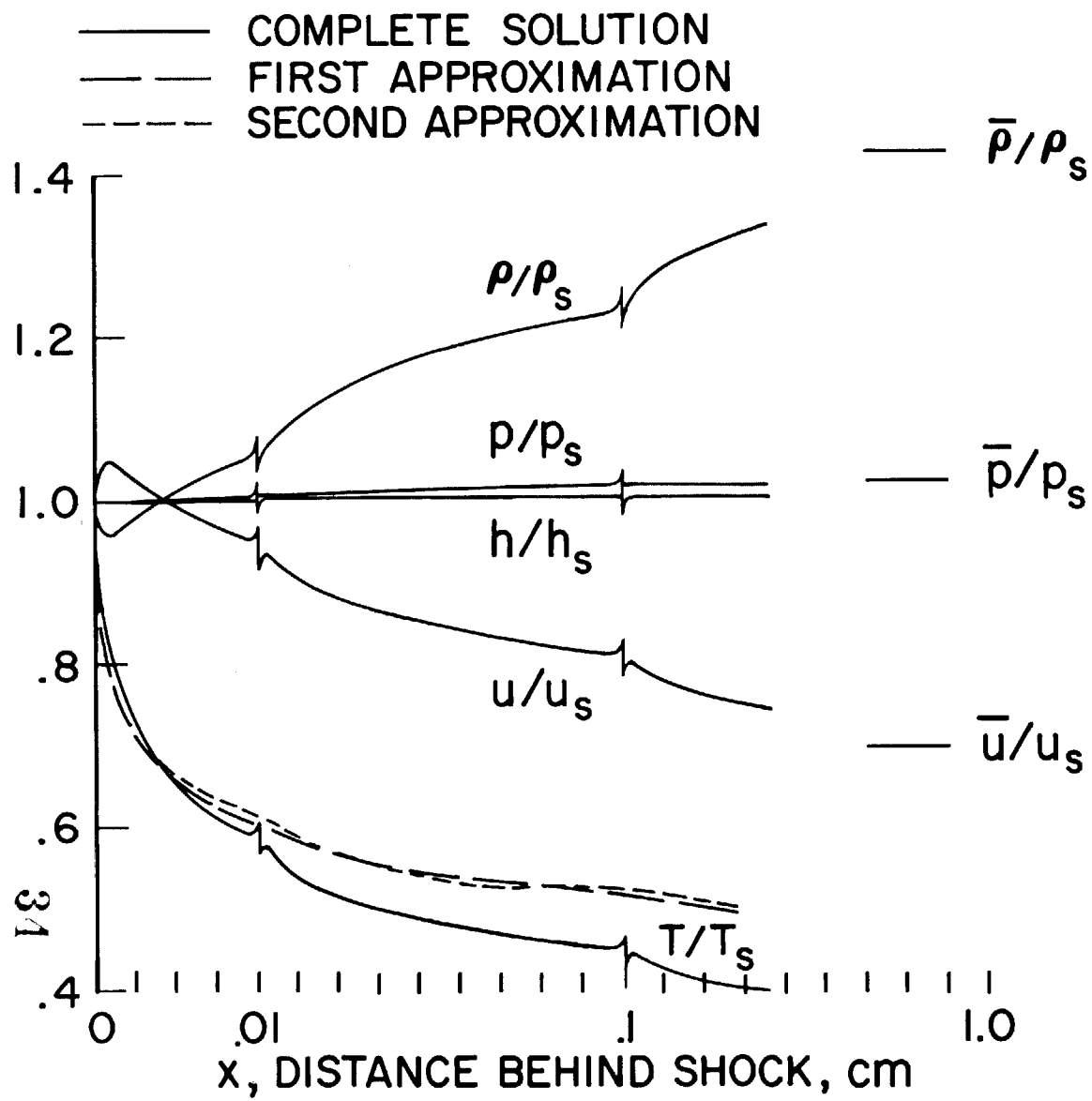

(a) Velocity and thermodynamic properties.

Figure 9.- Nonequilibrium flow-field profiles (u_∞ = 6 km/sec, $\rho_\infty/\rho_o = 10^{-2}$).

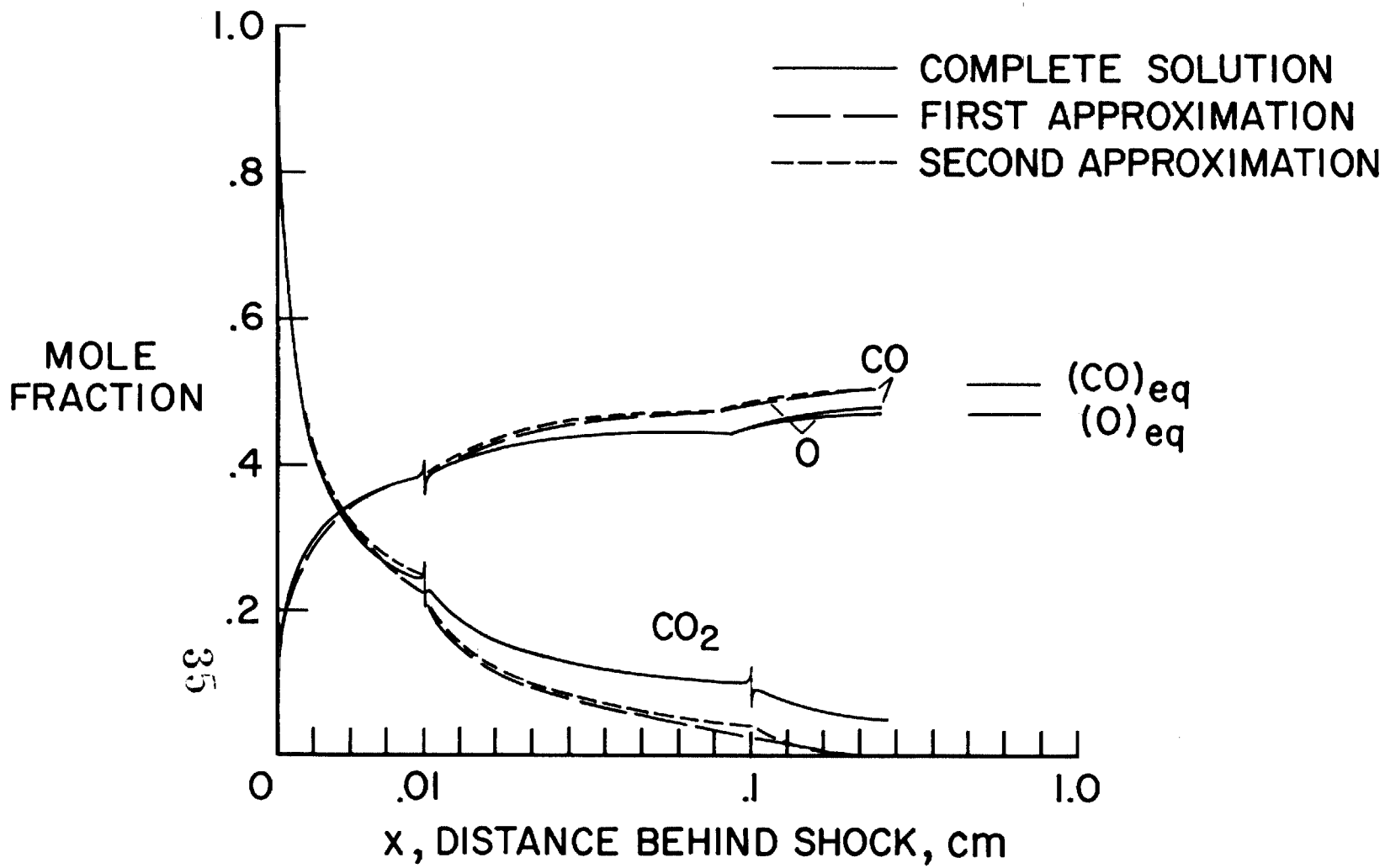

(b) Species concentration.

Figure 9.- Concluded.

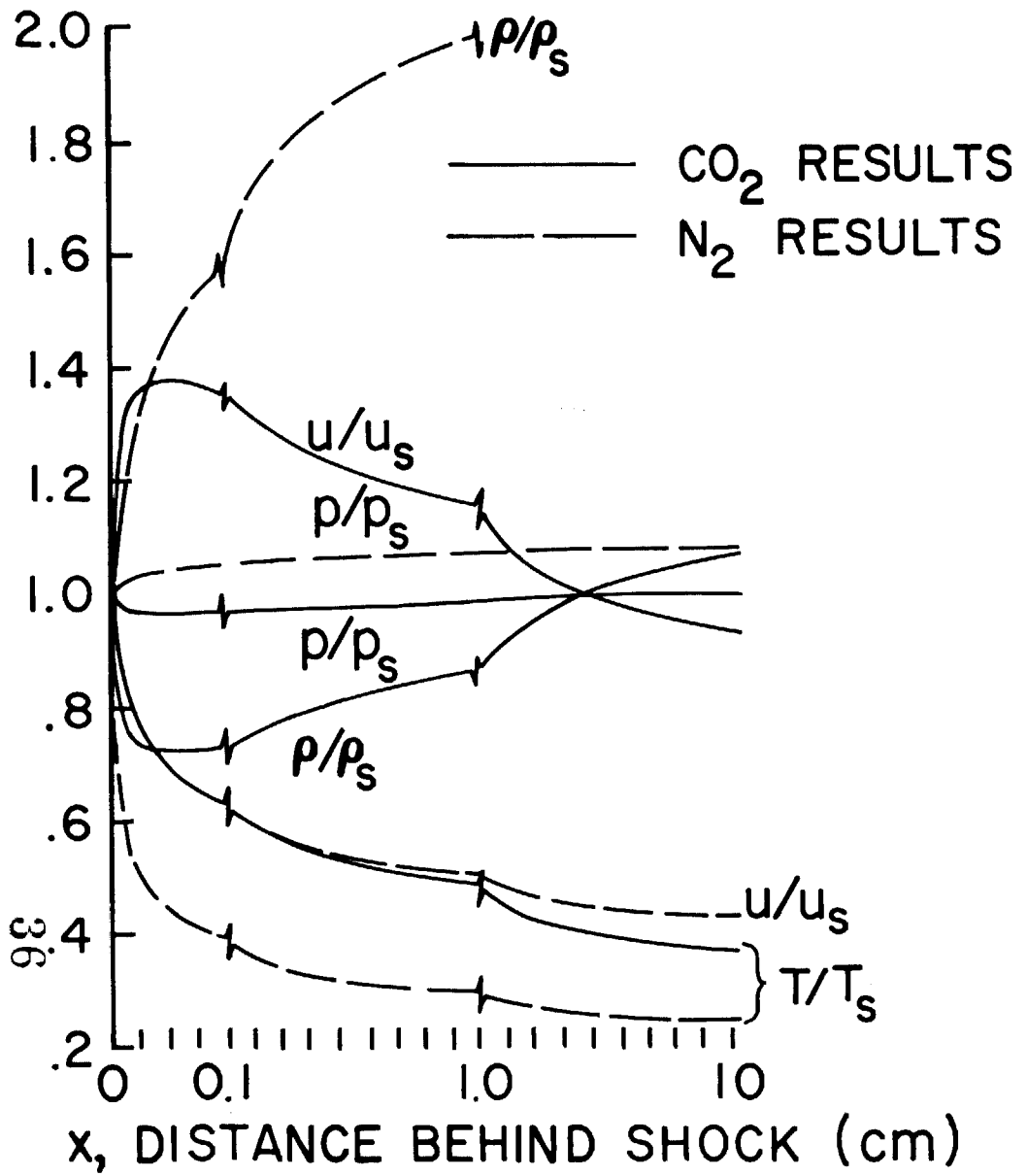

Figure 10.- Comparison between CO_2 and N_2 (u_∞ = 9 km/sec, $\rho_\infty/\rho_0 = 10^{-4}$).

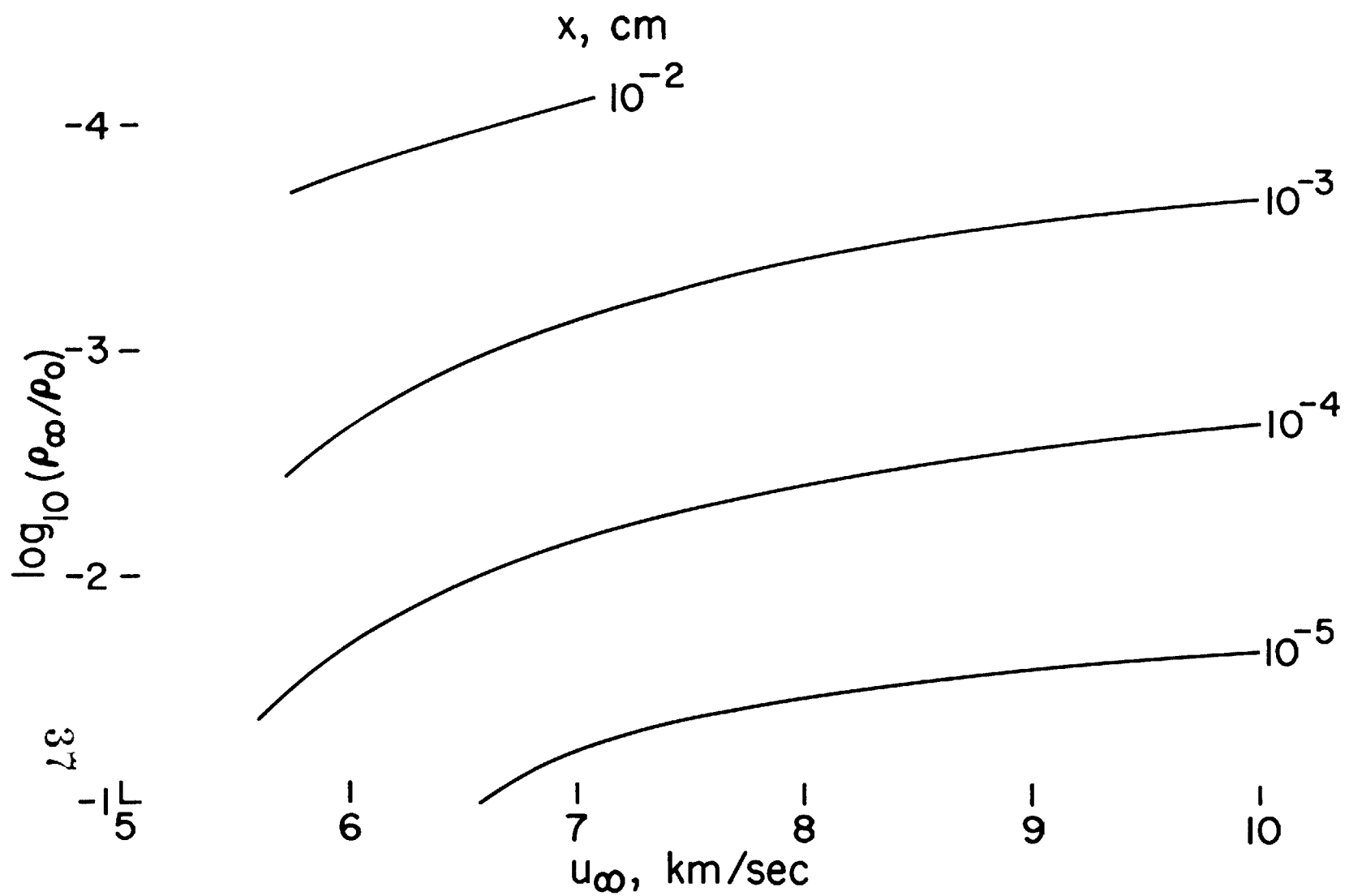

Figure 11.- Relaxation distance for 10-percent reaction completion.

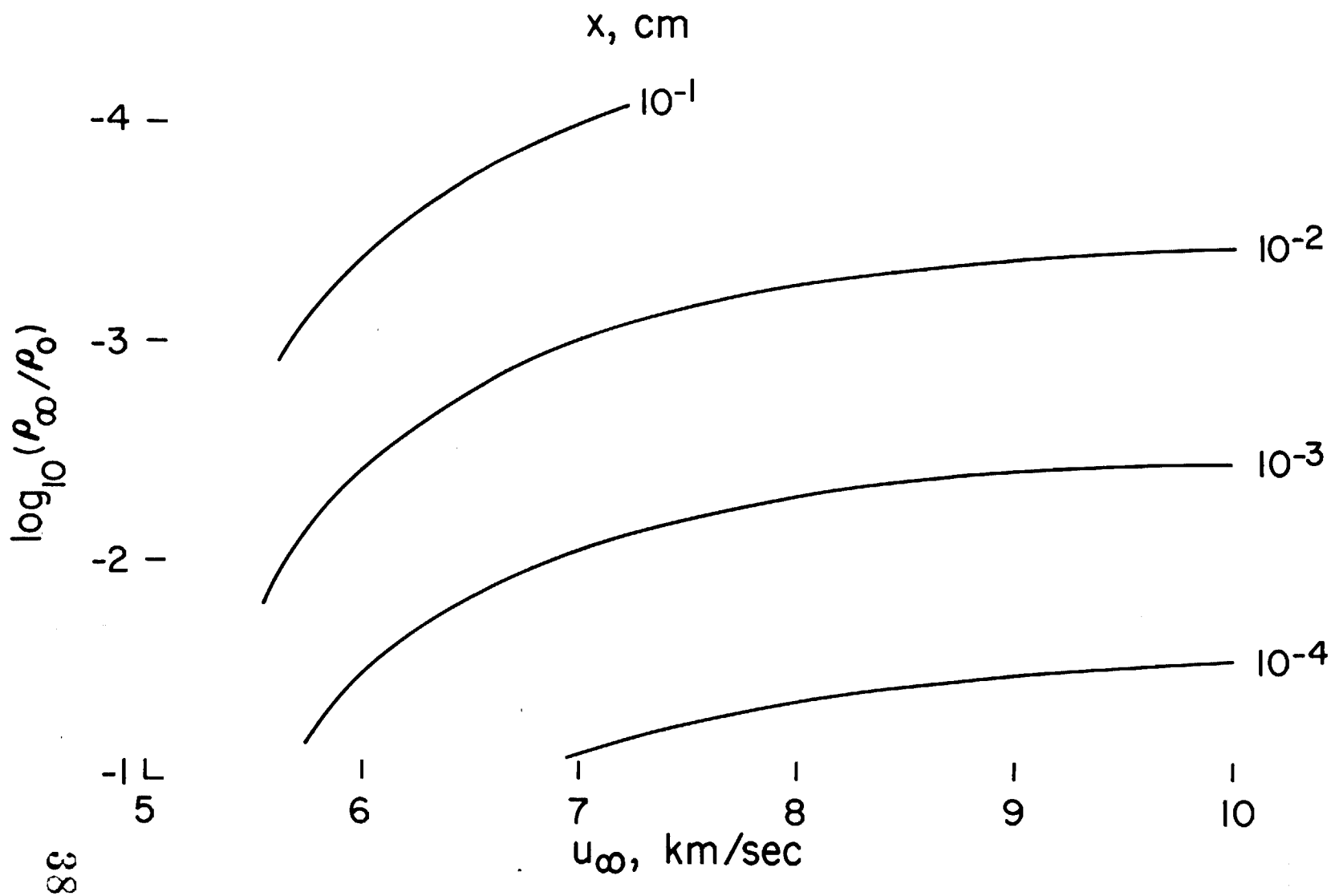

Figure 12.- Relaxation distance for 50-percent reaction completion.

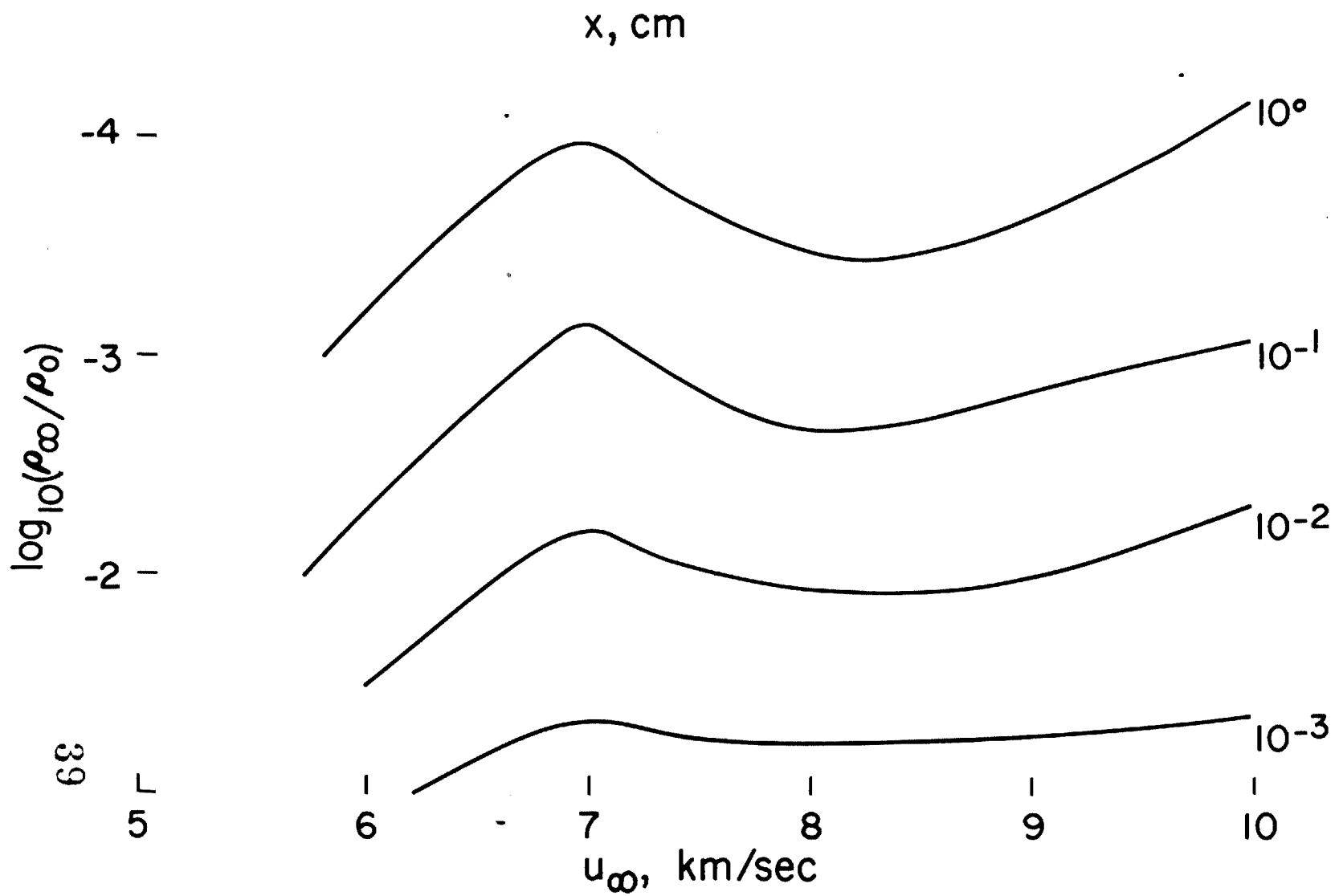

Figure 13.- Relaxation distance for 80-percent reaction completion.

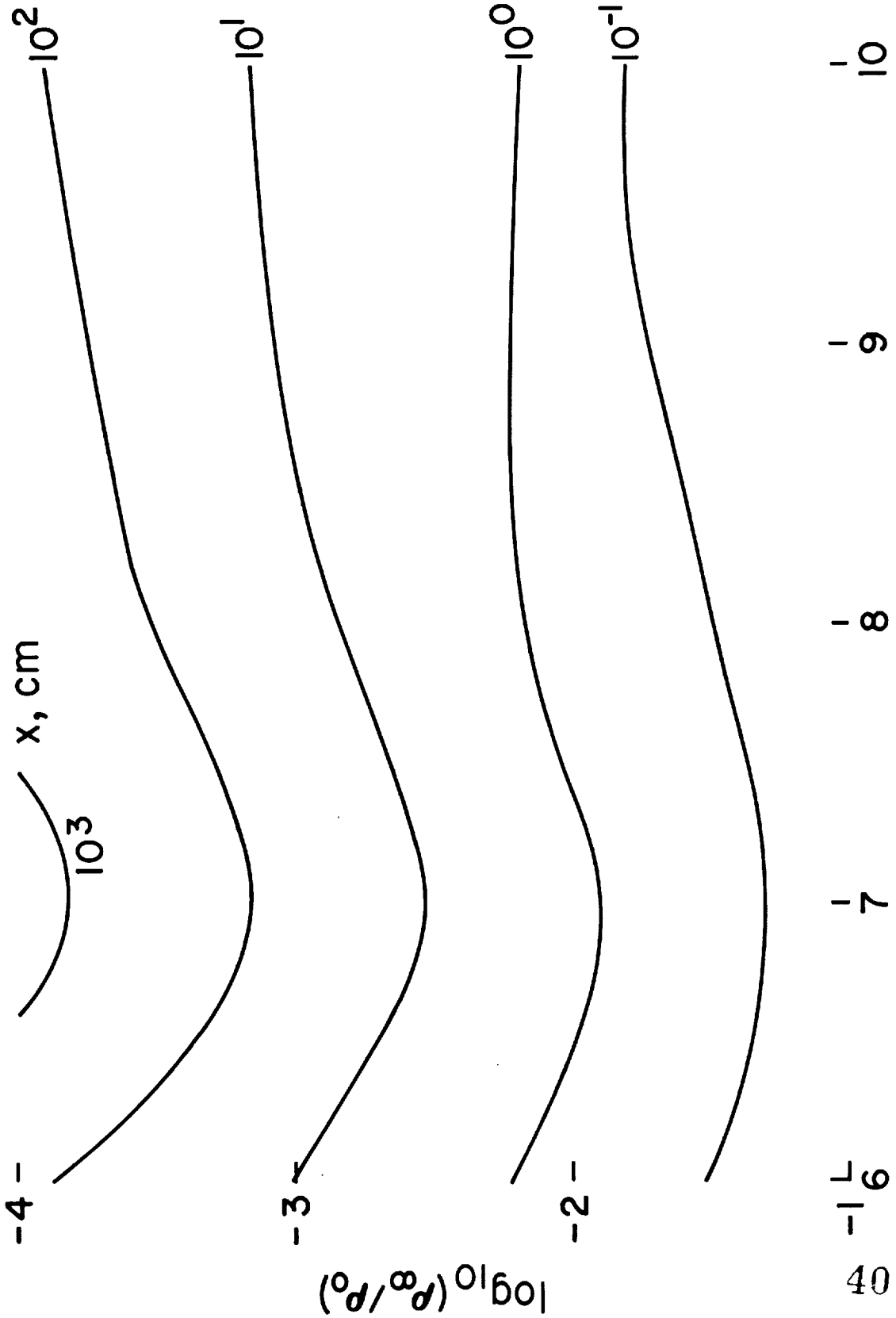

Figure 14.- Relaxation distance for 95-percent reaction completion.